TRIP A-2

Coastal Margin Interfluve Paleosols and their Stratigraphic Relationships with Tidally-Influenced Deltaic Deposits in the Sonyea Group (Frasnian) of Northwestern Delaware County, New York

Daniel Bishuk Jr.
EA Science and Technology
6731 Collamer Road
East Syracuse, New York 13057
danbishuk@eaest.com

Jon Hairabedian
New York City Department of Environmental Protection
West-of-Hudson Office of Engineering
P.O. Box 370
Shokan, New York 12481

James R. Ebert
Earth Sciences Department
SUNY College at Oneonta
Oneonta, New York 13820-4015

Introduction

The Catskill Clastic Wedge has been broadly subdivided into three magnafacies: Chemung, Cattaraugus and Catskill. These magnafacies have been interpreted as representing offshore, coastal/nearshore and terrestrial (fluvial) paleoenvironments, respectively. Of these magnafacies, the Cattaraugus has been the most poorly characterized and the nature of the Catskill shoreline has long been the subject of debate. Tectonic, eustatic and climatic processes interacted in complex ways to produce nearshore paleoenvironments in the Catskill Wedge which had aspects of both marine and terrestrial settings.

In this study, we describe tidally-influenced sediments of the Cattaraugus Magnafacies in parts of the Sonyea Group (Late Devonian, Frasnian) in Delaware County, New York (Fig. 1). However, our main focus is on paleosols in these strata as key features in understanding the complex nearshore environments which bordered the Catskill Sea. Several types of paleosols are documented, which yield insights into depositional and climatic processes at the Sonyea shoreline. More significantly, we show that paleosols, a typical feature of the Catskill Magnafacies, developed directly on sediments deposited under brackish, deltaic/estuarine conditions and on definitively marine sediments. In addition, many of the paleosols that we describe are immediately overlain by sediments deposited under marine or brackish conditions.

Such abrupt paleoenvironmental changes provide insights into processes of tectonic subsidence, eustatic changes in sea level and autocyclic processes, such as avulsion, which controlled the nature and position of the Catskill shoreline during Sonyea deposition.

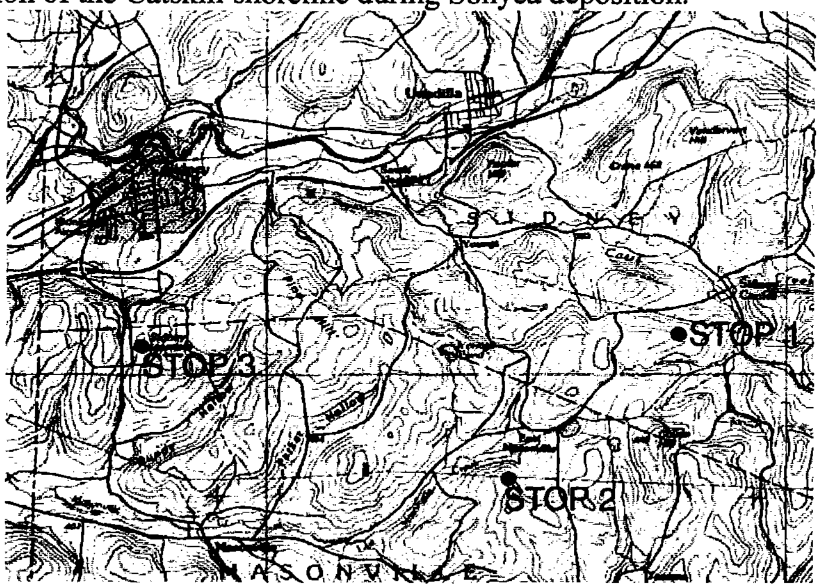

Fig. 1 Location map of field trip stops in the vicinity of Sidney and Sidney Center, New York. Sidney and Unadilla 7.5 minute quadrangles.

Chemung Magnafacies

The Chemung Magnafacies is defined as the fossiliferous rocks that represent the open-marine inner shelf. It comprises complexly interbedded sandstone, siltstone, and shale. Chemung stratigraphy is dominated by thick beds of sandstone and siltstone, separated by thin dark shales. Several authors have identified repetitive coarsening-upward sequences of mudstone through sandstone 15-30 meters thick within the Chemung Magnafacies in several other groups in the Middle and Upper Devonian (Craft and Bridge, 1987; Kirchgasser and others, 1994). In this study, two facies have been assigned to the Chemung Magnafacies. These are: 1) the dark gray shale facies, and 2) the hummocky cross-stratified facies. Continuous exposures of these facies are more abundant than rocks of the overlying Cattaraugus Magnafacies, but outcrops are still difficult to trace laterally.

Dark Gray Shale Facies (Facies S_{dg})

Facies S_{dg} occurs as uniform, dark gray shale and siltstone or as distinct interbeds within the hummocky cross-stratified facies with rare lenses of very fine sublitharenite. Planar bedding is most common in this facies. Discontinuous, ripple cross-lamination in sandy siltstone interbeds is cryptic, but occurs throughout the facies. These are interpreted as distal tempestites. Biogenic structures and invertebrates are absent in facies S_{dg}.

Discrete intervals of trough and wedge-shaped forms characterize this facies. Basal surfaces truncate underlying planar-laminated shale, and are overlain by a wedge of shale. Most of the truncation surfaces occur as solitary wedges, which overlie a sharp, concave-up discontinuity surface. The shale is inclined along the discontinuity surface and is in angular discordance with underlying planar beds. Inclination of shale decreases to sub-horizontal to horizontal planar laminations progressively upward within the wedges. Truncation surfaces also occur as facing pairs of intersecting, U-shaped troughs filled with shale that truncate each other. The shale that fills the U-shaped troughs is form concordant, and progressively flattens upward within troughs. Most wedges and troughs measure 5 to 20 meters in width, and truncate 1 to 2 meters of underlying shale.

Frasnian time experienced an overall rising sea level (Johnson, Klapper, and Sandberg, 1985), which is manifested in the Sonyea Group as numerous black shale tongues of facies S_{dg} that are probably coeval with drowned shoreface systems. Facies S_{dg} records three rapid transgressive pulses within an overall transgressive succession. Relative rapid sea-level rises associated with facies S_{dg} were apparently induced by a combination of epeirogenic lithospheric downflexure and differential subsidence (Quinlan and Beaumont, 1984), resulting in a rise in base level and trapping clastics in drowned estuaries, delta plains, and distal alluvial plain rivers (Marzo and Steel, 2000; Kirchgasser and others, 1994). The complete absence of invertebrates and biogenic structures, and the predominance of silt and clay in this facies indicate that deeper, anoxic conditions were introduced into formerly shallow areas.

The truncation surfaces that form shallow wedges and troughs are probably rotational gravity-slide failure scarps (Davies, 1977). Large quantities of unlithified sediment were disaggregated during liquefaction and removed by gravity sliding, owing to the fact that large-scale breccia, rotated blocks, or crumpled or other disturbed bedding structures are absent. The rotational slumps were probably triggered by storm events, overloading, or seismic activity.

Facies S_{dg} resembles descriptions of the Sawmill Creek Shale (Sutton, Bowen, and McAlester, 1970). However, we are reluctant to make this assignment because many shale intervals in the area meet the general description of Sutton and others (1970). Correlation of Sonyea black shale tongues (e.g., Montour, Sawmill Creek, Moreland) into the nearshore environments remains problematic.

Hummocky and Swaley Cross-Stratified Facies (H_{cs}) and Amalgamated Hummocky Cross-Stratified Subfacies (H_{cs}-A)

The Hummocky Cross-Stratified Facies is commonly interbedded with the dark gray shale facies. Hummocky cross-stratification is the dominant sedimentary structure in facies H_{cs} and shows striking similarities to examples cited by Craft and Bridge (1987), Halperin and Bridge (1988), Hamblin and Walker (1979), and McCrory and Walker (1986). Hummocky cross-stratified beds with wave-rippled caps are primarily found interbedded with siltstone and shale, but also occurs as amalgamated beds of very fine sublitharenite. Siltstone and shale interbeds are planar-laminated, blocky, or exhibit small-scale, cryptic and discontinuous ripple cross-lamination, and are commonly heavily bioturbated. Hummocky cross-stratified beds also occur as sheet-like sandstone beds with planar-lamination with lateral transition to hummocky cross-stratification similar to beds described by Halperin and Bridge (1988).

Hummocky cross-stratified beds have sharp erosional bases accompanied by soft sediment deformation. Directional sole marks such as flute and tool marks, coquinite layers, coquinite-filled scours, coquinitic hummocks or ripple forms, graded bedding and conglomerate are commonly found at the base of hummocky cross-stratified sandstones. Channel-filling sandstone bedsets, large sandstone pillows with kneaded surfaces, sandstone pillows with relatively undeformed strata, and gutter casts also occur at the base of sandstones in this facies. Additional details of structures and the diverse fossil assemblage present in facies H_{cs} are discussed in Bishuk, Ebert, and Applebaum (1991) and Bishuk (1989).

Hummocky cross-stratified intervals become increasingly amalgamated higher in the stratigraphic section (Subfacies H_{cs}-A*)*. A sharp, scoured and loaded contact with numerous ball and pillow structures and intraformational conglomerate occurs where amalgamated hummocky cross-stratification commences. Very fine and fine sublitharenite with rare conglomerate composed of shale and siltstone clasts are the dominant lithologies.

In amalgamated beds, concave-upward swaley surfaces pass laterally into convex-upward hummocky surfaces, thereby producing adjacent hummocks and troughs. Hummocks and swales are truncated laterally by hummocky cross-stratification or planar strata. Pebble lags commonly line these erosional surfaces. Most amalgamated beds are form-concordant, but discordant sets also occur. Structures, internal to amalgamated hummocky bedforms, include climbing ripples with steeply inclined axes of propagation (70 to 80 degrees) along the flanks of hummocks. The ripples generally show migration toward hummock crests. Hummocks and swales commonly contain several horizons of *Rhizocorallium* (?) burrows and sinuous epichnial trails of *Scalarituba*. Amalgamated hummocky beds rarely have distinct sole marks along erosional bases. Where present, sole marks include flute casts, load casts, and a variety of tool marks.

Fossils decrease markedly in abundance and diversity where amalgamated hummocky cross-stratification dominates the section. However, carbonized plant fragments are abundant. The most common fossil is the rhynchennelid, *Cupularostrum*. Other fossils, in order of decreasing abundance, include the bivalve, *Sphenotus*, the spiriferid, *Platyrachella*, other unidentifiable brachiopod fragments, fish fragments, crinoid ossicles, and the bivalve, *Cypricardella*. The fossils are most commonly found associated either with loaded scour and fill bases as coquinite shelly lags or within intraformational conglomerates.

Hummocky cross-stratification in the study area is interpreted as a storm-produced structure occurring below fair weather wave base and above storm wave base (Harms, 1975, and many others). The lower portion of the hummocky cross-stratified facies is therefore interpreted as representing deposition on a storm-dominated shelf. Similar interpretations have been made for other parts of the Chemung Magnafacies (Craft and Bridge, 1987; Halperin and Bridge, 1988).

The stratigraphic position of this facies, the predominance of fine sand, and a marked upward decrease in fauna suggest that the amalgamated hummocky cross-stratified portion of this facies occupies the lower shoreface. Siltstone and shale interbeds are rarely preserved, indicating that waves or currents (e.g., longshore-, tidal-, and storm-driven) had effectively winnowed the fine fraction (Swift, 1984). Paleoflow direction in this facies is consistently to the north, which may represent the longshore or geostrophic current direction. The marked decrease in faunal abundance indicates environmental stress associated with the nearshore zone (Thayer, 1974).

The hummocky cross-stratified facies is integrally involved in the overall progradation of the Catskill clastic wedge. Vertical upbuilding of hummocky cross-stratified beds at rates greater than the average rate of subsidence caused shallowing in the nearshore zone (Hamblin and Walker, 1979). Given the high volume of sediment delivered to the Catskill Sea, vertical upbuilding of hummocky beds was probably so rapid that accommodation space was consumed rapidly, thereby accelerating progradation rates of shelf and shoreface deposits. Progradation ceased when interrupted by rapid transgressive pulses and when tectonic conditions and/or the weight of nearshore deposits were sufficient to cause rapid subsidence. This is substantiated by hummocky cross-stratified beds overlying paleosols at outcrop 6. Since hummocky cross-stratification is chiefly deposited below fair weather wave base, relative sea level change must have risen by a minimum of 10-15 meters, which is attributable to a combination of eustasy and subsidence. Subsidence alone may not account for this disparity. A major river avulsion and/or a directional change in dispersal of sediment from the source area likely contributed to abandoned or diminished nearshore deposition, which would allow subsidence to outpace accumulation.

Cattaraugus Magnafacies

The Cattaraugus Magnafacies comprises the transitional rocks between obvious non-marine river channel and floodplain deposits of the Catskill Magnafacies and the obvious fossiliferous, open-marine deposits of the Chemung Magnafacies. Hence, the Cattaraugus Magnafacies is somewhat ambiguous in that it may possess aspects of both marine and non-marine environments (Linsley, 1994). An example of the intriguing, yet confusing nature of the Cattaraugus Magnafacies is the presence of channelized, fluvial-like deposits with marine shells at the base, which have been documented in several Upper Devonian studies (Johnson and Friedman, 1969; Bridge and Droser, 1985; Halperin and Bridge, 1988; and Bridge and Willis, 1991). In these examples, depositional environments change abruptly both laterally and vertically. These authors also note that marine and non-marine environments are separated by erosion surfaces where beach and intertidal facies might be anticipated. Within the Sonyea Group, we have documented multiple facies which offer new insights into the marine-brackish transition zone of the Cattaraugus Magnafacies. Regrettably, the transition between brackish and fresh water settings has not received additional clarification because no rocks that may be definitively assigned to the Catskill Magnafacies have been identified in this study area.

Shoreface deposition in the Cattaraugus Magnafacies is recorded by three facies. These are: 1) the trough cross-bedded facies; 2) the planar bedded multistorey sandbody facies; and, 2) the heterolithic bedded facies. Limited exposure has made reconstruction of facies relationships difficult. However, it is readily apparent at outcrops that the three facies are stacked in repetitive sequences. A survey of location and elevation of the outcrops using GPS as well as quarry activity in the last decade has helped to alleviate some of the difficulty in facies reconstruction (See Appendix I: listing of outcrops).

Trough Cross-Bedded Facies (T_{xb} – with Subfacies T_{xb}-td and T_{xb}-ti)

The trough cross-bedded facies (T_{xb}) consists of two subfacies, tidally-dominated subfacies (T_{xb}-td) and tidally-influenced subfacies (T_{xb}-ti), which are both assignable to an unnamed formation of the Cattaraugus Magnafacies. Subfacies T_{xb}-td occurs stratigraphically lower than subfacies T_{xb}-ti. Both subfacies are lithologically and structurally similar, but the sediment in subfacies T_{xb}-td is clearly differentiated into laminae of different well-sorted grain sizes and contains a greater abundance of tidally-produced sedimentary structures.

TIDALLY-DOMINATED SUBFACIES T_{XB}-TD

Subfacies T_{xb}-td consists of repetitive fining-upward sequences of moderately well sorted, fine sublitharenite. Sequences are separated by erosional scour surfaces and reactivation surfaces. Erosional surfaces are locally marked by a coarse sandstone- supported conglomerate and/or pebble lag. Clast lithologies are mainly siltstone and shale granules and pebbles, with rare calcrete clasts. Carbonized stems, branches and occasional logs are common at erosional bases and are locally abundant throughout the facies. Rare concentrations of invertebrates line the bottoms of troughs at and just above erosional bases at some outcrops. These concentrations are nearly monospecific, comprised of either the rhynchenellids *Cupularostrum* or *Camarotoechia* with rare crinoid ossicles. Trace fossils are restricted to rare occurrences of *Archanodon*-like, roughly cylindrical, nearly vertical burrows measuring 7-10 cm in diameter and up to 0.75 m long (Fig. 2). The caliber of the *Archanodon*-like burrows is consistent with *Archanodon* burrows identified by Bridge and others (1986), Gordon (1988), and Miller (1979). These burrows occur only at outcrops 7 and 21. No body fossils of *Archanodon* have been found.

Fig.2 Trough cross-bedded facies showing tidal drapes and coarse-fine bundling. An *Archanodon*-like burrow is present to the left of the scale.

Small- to medium-scale trough cross-bedding is the dominant sedimentary structure in the facies (Fig. 2). Many sets are sigmoidal in shape. The most striking and characteristic feature of subfacies T_{xb}-td is that the sediment on trough foresets is clearly differentiated into repetitive couplets of laminae of different well-sorted grain sizes. These couplets consist of fine sand alternating with very fine sand and silty mud drapes. Weathered outcrop surfaces commonly accentuate the alternating grain sizes, where finer grained drapes are weathered into recessed grooves adjacent to more resistant ridges of fine sand. Thick-thin alternations are observed in couplet bundle thicknesses on trough foresets. In addition, thickness variations in couplet bundles are also observed in some bottomset beds. Dip angles on trough foresets range from 10 to 25 degrees with an average inclination of approximately 15 degrees. Cross-beds commonly climb at low angles of propagation and are largely unidirectional, but locally are multidirectional. In general, the thickness of cross-bed set thins upward within the facies with reactivation surfaces become more common. In addition, dip angles on troughs decrease upward in the facies. Dune bedforms are uncommon. These sedimentary structures are strikingly similar to those described by de Mowbray and Visser (1984) and Nio and Yang (1991).

Some cross-beds contain normally graded, lenticular laminae with asymmetrical ripples and closely associated crinkled laminations, which oppose the dominant cross-bed paleoflow direction. The asymmetrical ripples migrate up the avalanche slope of dunes, occur in discrete units within the foresets, and are commonly bounded by very fine sand and silty mud drapes. Therefore, they clearly are not backflow ripples. In general, the asymmetrical ripples migrate from the base to the middle portion of foresets, and less commonly migrate to the crest of foresets. Paleocurrent directions obtained from trough cross-beds and asymmetrical ripples are dominantly northward, ranging from northwest to northeast. Asymmetrical ripples on dune foresets shows a subordinate southward paleoflow (southeast to southwest).

Some trough cross-beds are truncated by interbeds of fine sandstone that appear massive, bioturbated, and relatively structureless as compared to subjacent units. These interbeds are subhorizontal and of variable thickness. They pinch and bulge laterally and are bounded by recessively weathered grooves of very fine sandstone drapes. Some of these interbeds possess suspect, wavy crinkle laminations and crude bulges resembling starved ripples. The frequency of these massive interbeds increases upward in the facies.

Trough cross-beds are commonly intercalated with vertically-stacked, thinly-interlaminated couplet sequences of rhythmites consisting of fine sand with very fine sand drapes or very fine to fine sand with silty sand or silt-mud drapes (Fig. 3). These rhythmites are arranged as horizontal to subhorizontal planar lamination and gently inclined, long planar-tabular cross-beds (dip angles less than 5 degrees). Two types of lamina occur in couplet sequences. As defined by Williams (1991), simple laminae include only one sandy layer with one fine drape. Composite laminae, which consist of semilaminae embedded within simple laminae, are less common in the study area. Each simple lamina or semilamina is a graded layer 0.2 to 3 mm thick with a lower layer of fine sand passing upward into a thin band of silty sand or silt-mud. Double mud drapes also occur, but are uncommon.

Couplets appear to be unequal in thickness with a regular alternation of thick and thin couplets. These alternations are arranged in groups of thicker couplets with fine sand and very fine sand drapes and groups of thinner couplets with very fine to fine sand and silty mud drapes. In addition, the silt-sand rhythmites show a cyclical pattern where regular alternations of sand-poor packages and sand-rich packages can be identified at intervals of 17 to 22 cm. Rhythmites in the study area are similar to examples described by Nio and Yang (1991), Williams (1991), and Fenies and Tastet (1998). In general, planar-laminated interbeds become more common upward in the facies.

Contacts between subfacies T_{xb}-td and other facies units are covered throughout the study area. However, based on the distribution of closely-spaced outcrops, subfacies T_{xb}-td appears to occur consistently between facies H_{cs}-a and P_{bms}. At outcrop 21, the upper contact of T_{xb}-td with the overlying facies P_{bms} appears to be gradational. Subfacies T_{xb}-td is laterally traceable for approximately 7 miles from the east at outcrop 20 in Sidney Center to the south-west at outcrop 7 on Sidney Mountain. Estimated maximum thickness of subfacies T_{xb}-td is approximately 10-15 meters, based on moderately-spaced outcrops in Sidney Center.

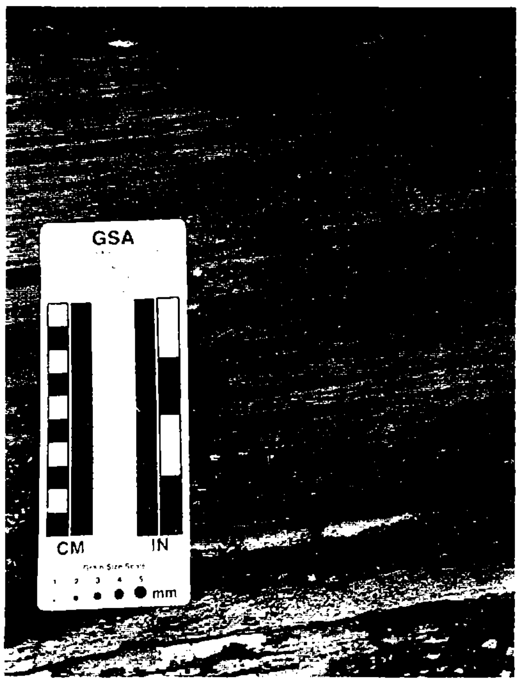

Fig. 3 Sub-horizontal gently inclined tidal rhythmites.

New observations from subfacies T_{xb}-td have been added to the data of Bishuk, Ebert, and Applebaum (1991), and now provide overwhelming evidence of tidal activity along the Frasnian paleoshoreline. The repetitive couplets of laminae of different well-sorted grain sizes are clear evidence of tides in subfacies T_{xb}-td (See also de Mowbray and Visser, 1984; Smith, 1988; and Nio and Yang 1991). The unidirectional nature of the trough foresets (i.e., paleoflow toward northwest) records a strongly asymmetric to asymmetric, ebb-directed tide. The asymmetrical ripples and closely associated crinkled laminations, which oppose the dominant paleoflow, represent flood-directed subordinate tidal currents.

It is unclear whether the large caliber vertical burrows with spreites found in subfacies T_{xb}-td were actually made by *Archanodon* or a bivalve with similar feeding and dwelling habits. The presence of *Archanodon*-like burrows in tidally-influenced deposits is intriguing, since it is widely accepted that *Archanodon* inhabited primarily fresh water fluvial environments (Bridge and others, 1986, Thoms and Berg, 1985). Thoms and Berg (1985) stated that the burrows are found only in nonmarine deposits near the Catskill paleoshoreline. Miller (1979) and Friedman and Chamberlain (1995) have suggested alternative interpretations that similar burrows occur in tidal channel and shallow subtidal deposits. Gordon (1988) states that if all of the structures that are currently called "large vertical (meniscate) burrows" have a common origin, then an explanation for their broad environmental range (from fully marine to clearly nonmarine deposits) is warranted. As a result, the burrows should not be interpreted as structures resulting from a "freshwater" bivalve. It is clear that the *Archanodon*-like burrows in the study area inhabited tidal channel and tidal flat locales. Since no body fossils have been found associated with the burrows and in subfacies T_{xb}-td, we cannot positively identify them as having been made by *Archanodon.*

Sedimentary structures in the study area indicate that sedimentation patterns near the Frasnian shore are more consistent with estuarine than deltaic processes. Trough crossbeds record deposition by migrating dunes within a laterally accreting, tidal inlet and tidal creek complex at or near the mouth of a tidally-influenced delta. These deposits formed across an area from the tidal inlet at the river mouth into the estuarine funnel and into protected tidal creeks nearest to the river mouth. This interpretation is supported by the predominance of sigmoidal trough cross-beds, evidence of current reversals with differing flow magnitude, a sparse marine fauna, and the stratigraphic position of this facies, between the multi-storey planar-bedded facies (upper flow regime sand flat deposits of the medial portion of the estuarine-like river mouth of the delta) and the underlying amalgamated hummocky cross-stratified facies (storm-influenced lower shoreface/proximal offshore deposits). Paleoflow was dominantly toward the north, with minor variations toward the northeast and northwest, which suggests that tidal inlets migrated in this direction. This northerly paleoflow may record the dominant storm track, the prevailing wind direction and longshore current, or dominant tidal flow. More detailed interpretation of these and other structures within this facies may be found in Bishuk, Hairabedian and Ebert (in preparation).

TIDALLY-INFLUENCED SUBFACIES T_{XB}-TI

Subfacies T_{xb}-ti is nearly identical to subfacies T_{xb}-td, but with a few important differences. Like subfacies T_{xb}-td, subfacies T_{xb}-ti consists of repetitive fining-upward sequences of moderately well sorted, fine sublitharenite. Small- to medium-scale, commonly sigmoidal trough cross-bedding is the dominant sedimentary structure. Trough cross-bedding is intercalated with horizontal planar lamination and gently inclined, long planar-tabular cross-beds with dip angles less than 5 degrees, which become dominant upward in the facies.

The most notable difference is that subfacies T_{xb}-ti rarely displays the repetitive couplets of laminae and associated differential weathering described above. Instead, very fine sand and silty mud drapes occur sporadically on asymmetrical ripples which migrated up the avalanche face of trough cross-beds. The asymmetrical ripples occur near the base and toe of foresets similar to those described by de Mowbray and Visser (1984) and Nio and Yang (1991). Rare occurrences of reformed ripples with small-scale herringbone cross-lamination are found at outcrop 42. The herringbone cross-lamination is confined to scours at the crests of ripples marked by reactivation surfaces. These reformed ripples display asymmetry opposite the dip direction of the primary cross-lamination within the ripple.

The basal contact of T_{xb}-ti with underlying paleosols is visible at outcrops 43, 47, and 53 (Figs. 4, 5). The contact is sharp, planar, and non-erosive (e.g., the A horizon in underlying paleosols is preserved), but when traced laterally across the outcrop, the contact becomes locally erosive with channel forms up to 0.5-0.75 m deep. Medium to coarse sand-supported conglomerate and/or pebble lags measuring up to 0.3 m thick overlies the contact. Clast lithologies are mainly siltstone, shale, and calcrete granules and pebbles. Locally, the basal contact and base of trough cross-set boundaries are spectacularly ornamented with flute casts and tool marks. Although paleocurrents from flutes show a dominant northeast to northwest azimuth, the basal contact at outcrop 43 has flutes which are oriented to the southeast. In addition, small dunes with trough cross-stratification immediately overlying the basal contact at outcrop 43 also bear consistent southeasterly azimuths. At outcrop 53, conglomerate-filled channel forms cut into trough and planar, tabular cross-strata. These concave-up channel forms measure up to 1.5 meters deep and 5-10 meters wide.

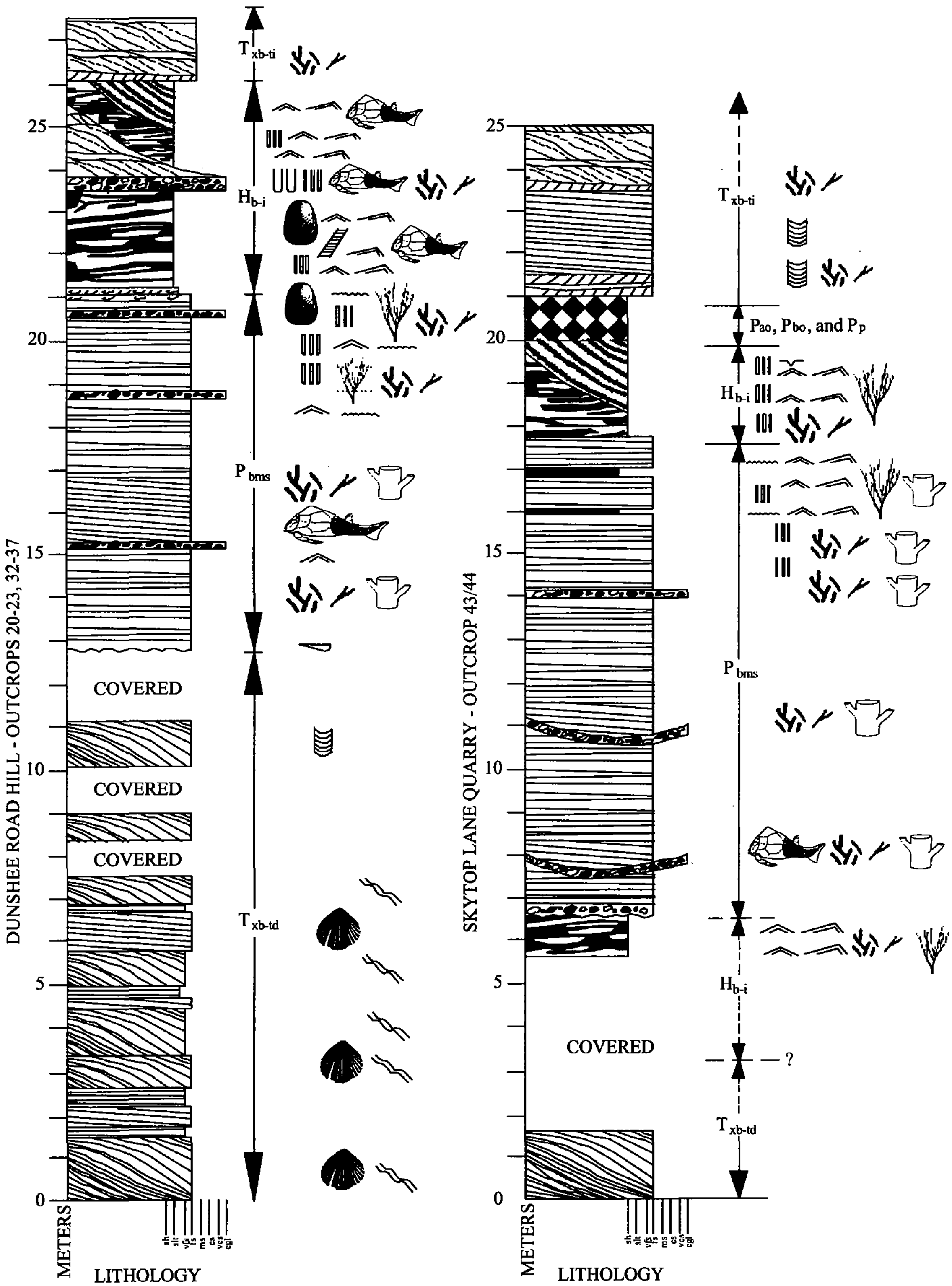

Fig. 4 Simplified stratigraphic columns for outcrops on Dunshee Road Hill and Skytop Lane Quarry (STOP #1).

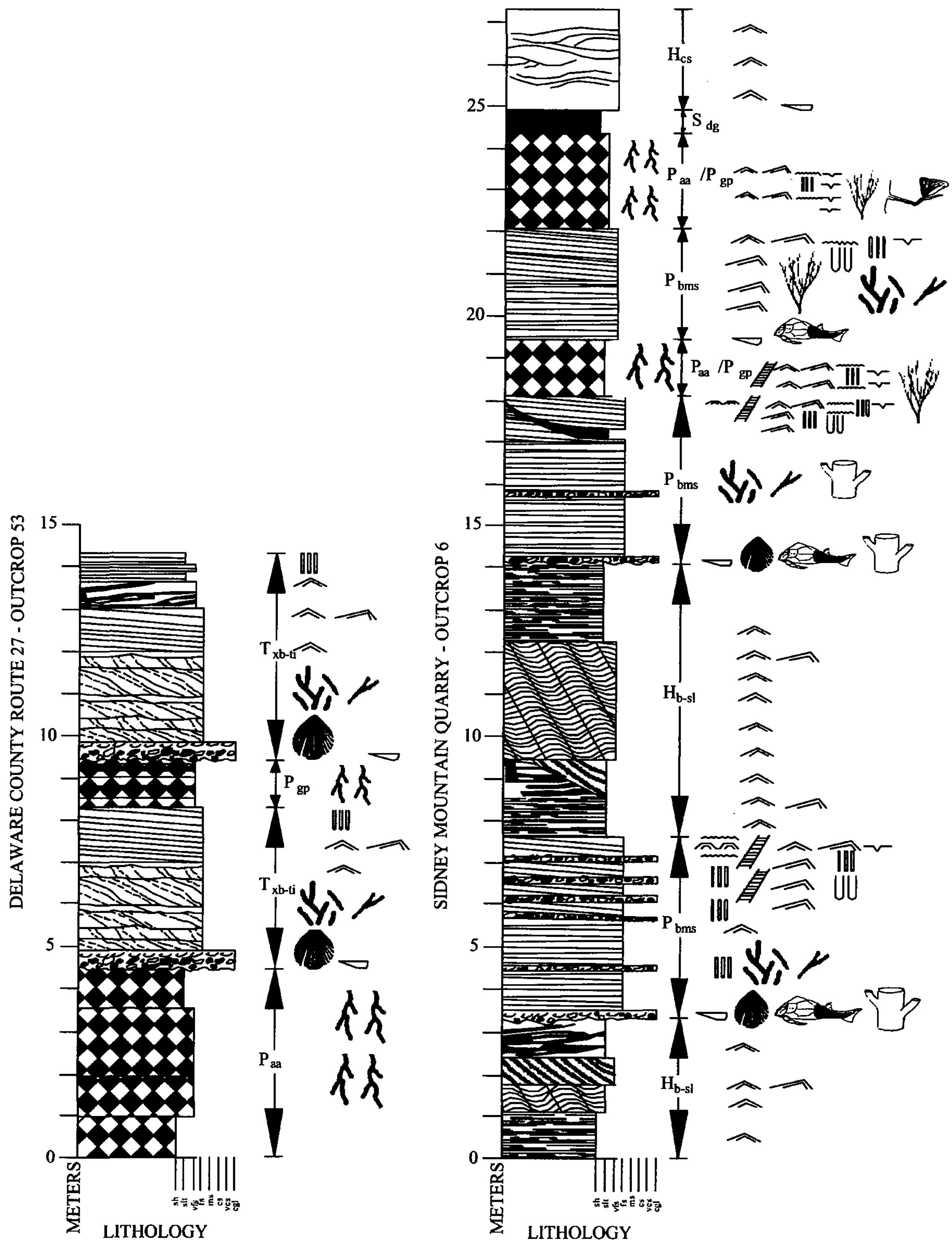

Fig 5. Simplified stratigraphic columns for Outcrop 53 and Sidney Mountain Quarry (STOP #3)

Explanation for Figures 4 and 5

LITHOLOGY

sh = Shale/Mudstone
slt = Siltstone
vfs = Very Fine Grained Sandstone
fs = Fine-Grained Sandstone
ms = Medium-Grained Sandstone
cs = Coarse-Grained Sandstone
vcs = Very Coarse-Grained Sandstone
cgl = Conglomerate

SEDIMENTARY & BIOGENIC STRUCTURES

- Shale/Mudrocks (Mudstone and Siltstone)
- Streaky Lamination/Lenticular Bedding (Undifferentiated)
- Flaser and Wavy Bedding (Undifferentiated)
- Flat Heterolithic Bedding
- Inclined Heterolithic Bedding
- Intercalated Inclined and Flat Heterolithic Bedding
- Planar Lamination
- Subhorizontal Planar Tabular Cross-Strata
- Trough Cross-Bedding (Ebb-directed)
- Trough Cross-Bedding (Flood-directed)
- Trough Cross-Bedding with Silt/Mud Drapes (Ebb-directed)

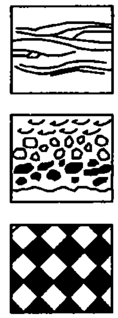

- Hummocky Cross-Stratification
- Sparse Shell Lag
  Extraformational Pebbles
  Intraformational Pebbles
  Erosion Surface
- Paleosol

- Symmetrical ripples
- Flat crested ripples
- Ladderback ripples
- Asymmetrical ripples
- Climbing asymmetrical ripples & crinkle laminations (oppose dominant cross-bed direction)
- Runzel marks
- Mudcracks
- Directional Tool Marks
- Large diameter _Archanodon_-like burrows with spreites
- _Arenicolites_ burrows
- Vertical _Skolithos_ burrows
- _Cupularostrum_ (Rhychonellid Brachiopod)
- _Barroisella_ (Inarticulate Brachiopod)
- _Bothriolepis_ Fish Fragments
- In Loco Plants (Minimally Transported)
- Transported Plant Fragments
- Wood, Branch, and Bark Fragments (Transported)
- Root Traces and Rhizoliths
- _Drapanophycus_ plant remains

Carbonized stems, branches and logs are common along erosional bases and are locally abundant throughout the subfacies. Concentrations of *Cupularostrum* and very rare crinoid ossicles occur at and just above erosional bases of two sequences of subfacies T_{xb}-ti at outcrop 53. No other invertebrates occur in subfacies T_{xb}-ti. Large caliber, *Archanodon*-like burrows are relatively uncommon, but occur at outcrops 43, 45, and 47. No other trace fossils have been observed.

Subfacies T_{xb}-ti abruptly overlies paleosols P_{ao}, P_{bo}, P_p, P_{aa}, and P_{gp} at several outcrops (Fig. 6). This contact is sharp, planar, and non-erosive (e.g., the A horizon in paleosols are preserved), but is locally minimally-erosive with channel forms. The upper contact of T_{xb}-ti is seen only at outcrop 53, where it is gradationally overlain by paleosol P_{gp}. At outcrop 53, both contacts are exposed and subfacies T_{xb}-ti is about 4-5 meters thick. Regional correlation of closely spaced outcrops indicates that subfacies T_{xb}-ti may reach thicknesses of 5-10 meters. Subfacies T_{xb}-ti is laterally traceable for approximately 3.5 miles from the southeast at outcrop 53 in Sidney Center to the west at outcrop 47 in East Masonville.

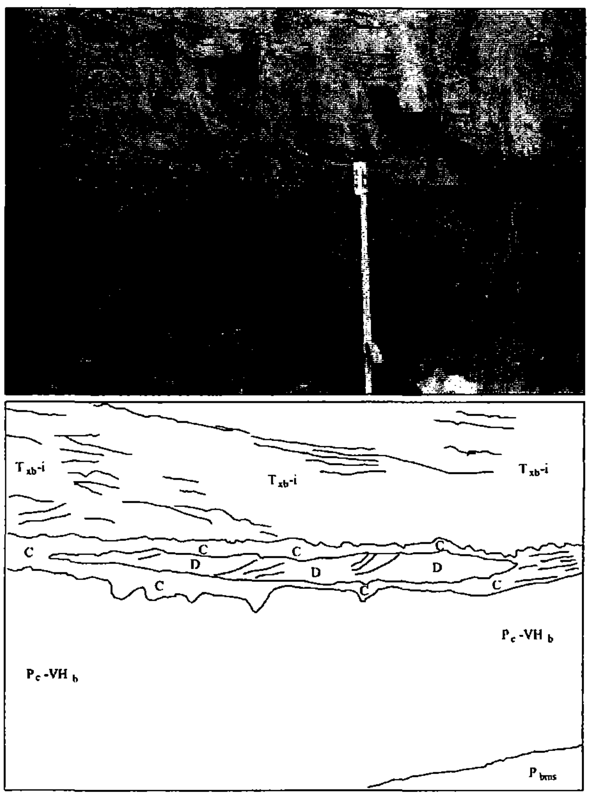

Fig. 6 Field photo and trace showing trough cross-bedded, tidally-influenced facies overlying paleosol (C and VH_b horizons). Note relict dune (D) within C horizon.

Sedimentary structures in subfacies T_{xb}-ti, such as sigmoidal trough cross-stratification, asymmetrical ripples migrating up the avalanche face of trough cross-beds, and reformed ripples with small-scale herringbone cross-lamination indicate mild tidal activity. The dominance of a northwest paleoflow is consistent with a very strong to strong asymmetric, ebb-directed tide (de Mowbray and Visser, 1984; Nio and Yang, 1991). The subordinate flood current was weak, since reactivation surfaces, flood-directed ripples, and mud drapes are rare. The presence of *Archanodon*-like burrows in subfacies T_{xb}-ti further supports the notion that these organisms occupied brackish water settings.

The basal erosion surfaces of subfacies T_{xb}-ti are inferred to be sequence-bounding unconformities, since subfacies T_{xb}-ti invariably overlies subaerially exposed lowstand surfaces comprising paleosols and other nonmarine environments. The differential erosion into underlying units observed at the basal contact of subfacies T_{xb}-ti reveals important clues to the nature of the marine transgressive surface. When traced laterally, the basal contact lacks significant relief indicating gentle onlap of marine waters into a series of antecedent coastal-plain vacuities such as paleosol-bearing interfluves and coastal drainage networks (i.e., drowned valleys and embayed coastline). Where the basal contact is sharp, planar, and non-erosive paleosol-bearing interfluves were apparently drowned in place. Where the contact becomes locally erosive with channel forms up to 0.5-0.75 m deep, the transgressing shoreface preferentially scoured antecedent fluvial and distributary channels of the paleovalley. The resultant erosion surface is therefore characterized by little or no microtopography on the paleolandscape flooding surface and lack of coastal plain incision. Similar marine transgressive surfaces, resulting in drowned, broad shallow valleys or embayed coastlines, have been described by Abbott (1998), Ricketts (1991), and Okazaki and Masuda (1995). No incised valley fill systems, and lowstand systems tract (LST) fluvial deposits and transgressive systems tract (TST) marine deposits associated with them, have been identified in the study area.

The basal erosion surfaces of subfacies T_{xb}-ti represent ravinement surfaces produced by transgressive flooding. Flute casts on the contact and small-scale trough cross-stratified dune bedforms immediately overlying the contact are oriented consistently to the southeast. This is not the orientation that would be expected if subfacies T_{xb}-ti were fluvial. Instead, the paleoflow data indicate onshore-directed (flood) tidal currents. The transgressive successions were deposited within and seaward of the erosional shoreface, starting with fields of shell-bearing gravel lags at the basal contact. These shell-bearing gravel lags are interpreted as winnowed and transported lag deposits of LST coastal plain and TST paralic facies that were consumed by erosion at the transgressing shoreface and, at least in part, redeposited offshore. Similar shell-bearing gravel lags are documented by Abbott (1998).

Planar-Bedded Multistory Sandbody Facies (Facies P_{bms})

The planar-bedded multistory sandbody facies (P_{bms}) consists of moderately to well sorted, very fine- to fine-grained sublitharenites (Fig. 7). Planar beds are horizontal or subhorizontal. Horizontal beds locally attain a thickness of 7 meters. Bedding plane partings average 2 to 6 centimeters in thickness. Internal lamination is subtle and detectable only in thin section and polished slabs. Inversely graded laminae are rare. Upper stage planar laminations are abundant. Structures such as parting lineation and aligned carbonaceous plant fragments show a dominantly NW-SE paleocurrent direction at all localities. Vertical, hematitic burrows of *Skolithos* occur at several locations. Abundant inarticulate brachiopods of *Barroisella campbelli*(?) and *in loco* (i.e., minimally transported) delicate plant leaves and stems occur as a lag on the top surface of facies P_{bms} at two outcrops. *Barroisella campbelli* (?) occurs with root casts, carbonate-filled and open void rhizoliths, and sandy rhizocretions at outcrops 24 and 25.

Horizontal planar beds are locally replaced laterally by subhorizontal, planar-tabular cross-strata and channel forms measuring 2-10 m wide and 1-2 m thick. Planar-tabular cross-strata are inclined less than 5 degrees and measure tens of meters in length and 1-4 m thick. Dip directions of these cross-strata are predominantly west to northwest. Channel forms are infilled with cross-bedded sandstone and occur near the top 1-3 meters of facies P_{bms}. Reactivation surfaces with flat shale intraclasts also display valves of *Cupularostrum* and *Platyrachella*, and fragments of the fish *Bothriolepis*, a fauna indicative of brackish conditions (Thayer, 1974). Highly abraded, arthropod fragments (trilobites or ostracods?) occur locally, as do flaser and wavy bedding with sand-filled mudcracks. Some bedding planes display trains of straight crested, asymmetrical ripples which have rounded to flat, planed-off crests. Other structures include symmetrical ripples, "ladder-back" ripples, and runzel marks.

Bedding planes are commonly strewn with carbonized and pyritized plant fragments, small branches, bark and rare logs (Fig. 8). Plant-rich strata commonly have yellow limonitic and reddish-orange hematitic stains from oxidation of pyrite. Discrete beds of intraformational conglomerate, consisting of flat shale clasts and weathered calcrete clasts occur on some bedding surfaces as well. These conglomerate beds occur more commonly as non-erosive sheets, and less commonly as low and broad erosive reactivation scour depressions measuring several meters wide and long and less than 10 centimeters deep, and channel lags measuring up to 1 meter deep. These scour depressions commonly contain mud drapes and abundant burrows of *Skolithos*(?), *Diplocraterion*(?), and *Paleophycus*(?). Large caliber, *Archanodon*-like vertical burrows are rare, occurring only at only two outcrops. Some localities display *Cruziana* trails, crescent-shaped burrows, *Rhizocorallium* (?), and "figure-8" burrows.

Facies P_{bms} is typically interbedded with the heterolithic-bedded facies (H_b). Vertical exposure of P_{bms} and H_b stacks is limited, so the contact of facies P_{bms} with the underlying facies T_{xb} is rarely exposed. Observed thicknesses of available outcrop exposures of P_{bms} and H_b stacks range from 6-15 meters (1-2 complete stacks present) up to a maximum of 25 meters (4 complete stacks present) in the continuous exposure at Sidney Mountain quarry (outcrop 6).

Facies P_{bms} is interpreted as upper-flow-regime (UFR) sand flat deposits accompanied by a drainage network of tidal channels and tidal point bars within a central, seaward-flaring estuarine-like funnel of a tidally-influenced delta. Sandy tidal flats occupied the margins of the estuarine-like funnel. The UFR sand flats are represented by the thick accumulations of horizontal planar-laminated beds. The thickness of horizontal planar-laminated beds (i.e., up to 11 meters at outcrop 43) is not surprising, since they were deposited in the zone of turbidity maxima, where tidal and sediment-laden fluvial currents intersected. The tidal channels are recorded as channel forms infilled with cross-bedded sandstone, whereas the tidal point bars are recorded as subhorizontal, planar-tabular cross-strata interpreted as lateral accretion surfaces. Sandy tidal flats are recorded by abundant tidal sedimentary structures found capping facies P_{bms}.

The sandstone bodies of facies P_{bms} are organized into erosional-based storeys with lateral-accretion bedding that are similar to other deposits interpreted as tidal bars in laterally migrating estuarine channels. Paleocurrent measurements indicate a dominant southeast to northwest flow, which coincides with the axis of the seaward estuarine mouth of the deltas. The paleoshoreline is oriented normal to this, in a northeast-southwest direction. This orientation is in agreement with past paleogeographic reconstructions of the Catskill Sea (Haeckel and Whitzke, 1984; Barrel, 1913, 1914). Similar ancient examples from other parts of the Catskill Clastic Wedge are reported by Slingerland and Loule (1988), Bridge and Droser (1985), Halperin and Bridge (1988) and, Bridge and Willis (1994). Griffing and others (2000) report similar facies from Gaspé and Dalrymple and others (1992) cite modern examples which appear analogous.

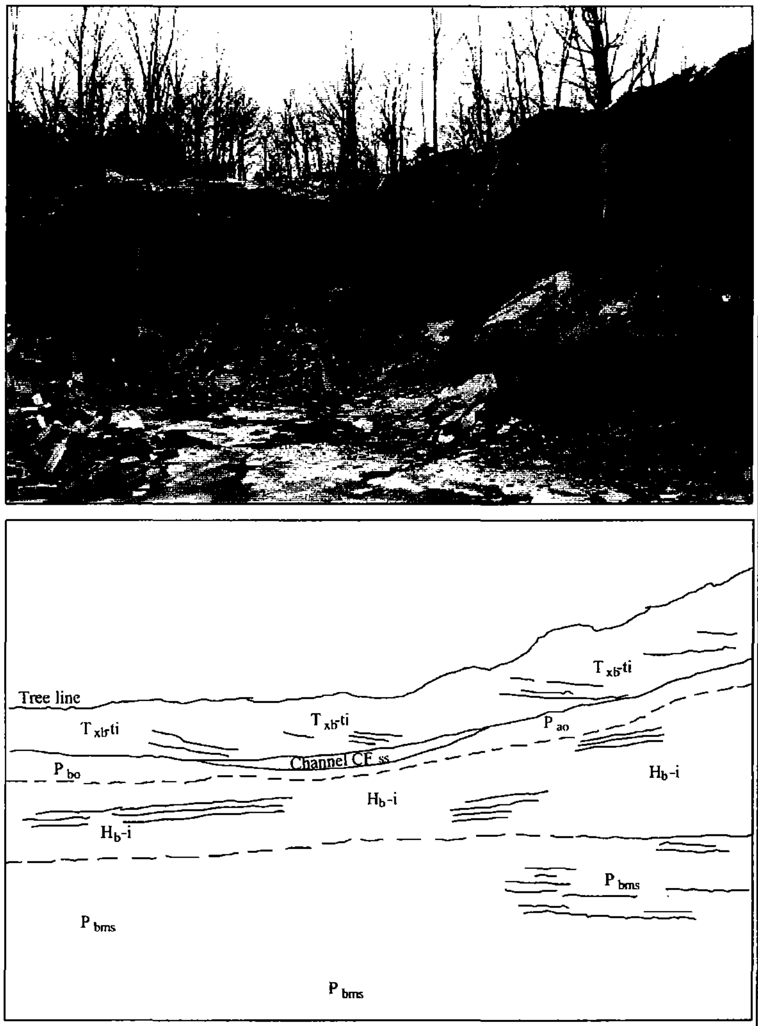

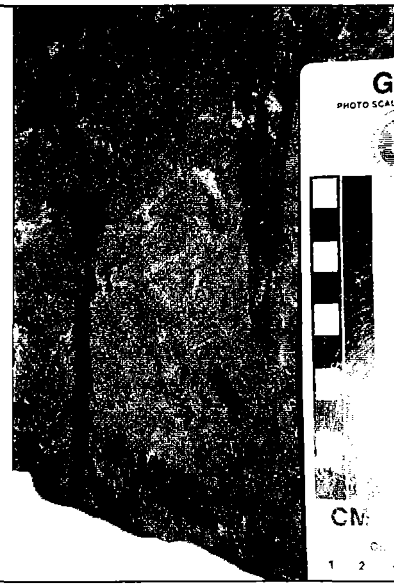

Fig. 7 (left) Planar bedded, multistory sandstone facies at the base of the outcrop. This facies is commonly mined as "bluestone." Relationships with overlying facies and paleosols is shown on trace.

Fig. 8 (above) Delicate plant debris strewn on bedding plane of planar bedded multistory sandstone facies.

Heterolithic-Bedded Facies (Facies H_b – with Subfacies H_b-I and H_b-SL)

The heterolithic-bedded facies (H_b) is comprised of two subfacies: inclined heterolithic bedded subfacies (H_b-I) (Fig. 7) and streaky-laminated heterolithic subfacies (H_b-SL). Facies H_b is invariably found interbedded as repetitively-stacked sequences with facies P_{bms}. Contacts with underlying facies P_{bms} are sharp and planar. This contact is locally erosional with facies H_b filling channel forms that are incised up to 4 meters into the underlying facies P_{bms}. Facies H_b is either gradationally overlain by paleosols or sharply overlain by facies T_{xb} and P_{bms}. The contact between H_b and T_{xb} is sharp, planar, and non-erosive, but is locally erosive with channel forms that incise up to 0.5-1 meter into the top of facies H_b. Facies H_b ranges in thickness from 1.2 to 6.8 meters at individual outcrops.

Heterolithic bedded subfacies (H_b-I)

Subfacies H_b-I is characterized by inclined heterolithic stratification (IHS) and inclined stratification (IS) as defined by Thomas and others (1987) and horizontal planar rhythmic bedding (i.e., flat heterolithic bedding or FHB), which bear some similarities to bedding described by Van den Berg (1981), Smith (1985), and Coleman, Gagliano, and Webb (1964). IHS and FHB are commonly intercalated, but one form may dominate at individual outcrops. Average inclination of IHS in the study area is approximately 7^{o} with an overall range from 3-25^{o}. Average inclination of IHS at outcrops where FHB predominates is 3^{o} or less. These stratification types consist of distinct cm-scale coarse- and fine-grained members that together constitute repetitive coarse-fine couplets.

Coarse members of couplets are predominantly homolithic, but may also contain one or more of the following: pebble- to granule-grade intraformational and extraformational conglomerates, carbonized wood and bark debris, and fish plates, bone fragments, and teeth of *Bothriolepis* and possibly *Eustenopteron*. Sandy members are generally consistent in thickness (i.e., 3-5 cm), but have an overall range in thickness from approximately 1-15 cm. Fine members of couplets are invariably heterolithic. Silty fine members are typically comprised of 1-3 cm thick layers, but mm-scale layers are also found. Lithologies are very fine to fine sublitharenite capped by sandy siltstone, siltstone, or mudstone. Fine members may also be intricately interlaminated (1-2 mm scale) with siltstone, mudstone, and carbonaceous plant detritus or, *in loco* plant fragments. These interlaminated fine members resemble horizontal pinstripes similar to the streaky lamination of subfacies H_b-SL.

Sedimentary structures common in coarse members include planar lamination and small-scale asymmetrical, symmetrical, and climbing ripple cross-lamination. Small- to medium-scale trough and planar cross-lamination is less common. Load and flute casts are common on the sole of sandy coarse members. Fine members are typically parallel-laminated, small-scale symmetrical and asymmetrical ripple cross-laminated, and lenticular-, flaser-, and wavy-bedded. Runzel marks are common on top bedding surfaces of coarse and fine members and are found in close proximity to mudcracks where they occur. Mudcracks occur throughout subfacies H_b-I, but are rare and closely associated with the top of channel fills. Asymmetrical ripples with superimposed mudcracks and ladder-back ripples are fairly common, and tend to occur near the top of subfacies H_b-I and within channel fills. Evidence for bidirectional paleoflow is rare, and is limited to ladder-back ripples.

Carbonized, pyritized, and chalcopyritized plant, wood, and bark fragments are commonly strewn on bedding planes in subfacies H_b-I. Rare carbonized impressions of shrub-like plants have also been found. These plant and woody fragments are typically oriented in a west-northwest to east-southeast paleoflow direction. Body fossils of invertebrates are extremely rare, consisting of sparse occurrences of *Barroisella campbelli*. Vertebrates are restricted to fish plates, bone fragments, and teeth of *Bothriolepis* and possibly *Eusthenopteron* found at the base of sandy IHS coarse members. Concentrations of fish bones average 3-8 centimeters in thickness (Figs. 4, 5). Gordon (1988) and Blieck (1982, 1985) described similar fish bone beds in other

Devonian marginal marine deposits. Two fish bone beds are laterally continuous for at least 100-150 meters. The lowermost bone bed at outcrops 35 and 36 changes laterally into a granule- and pebble-grade conglomeratic sandstone approximately 5-10 centimeters thick and 10-20 meters wide. The layer contains weathered siltstone, shale, and calcrete clasts. The conglomeratic sandstone is in turn traced lateral into a wedge-shaped point bar sandstone. This point bar sandstone is 1-1.5 meters thick and contains long sigmoidal-shaped inclined strata. Abundant, U-shaped *Arenicolites* burrows are found in the basal 30 cm of the sandstone. Two, articulated shells of *Archanodon* were found nearby in the float.

An overall vertical fining upward trend is evident at all IHS-bearing outcrops. Lateral fining away from channel forms (i.e., predominantly IHS-filled) into predominantly FHB is observed at some outcrops. The northeast portion of outcrop 43 contains lateral fining into a large abandoned channel (i.e., 4 meters deep and 20+ meters wide), which was subsequently plugged with predominantly IHS fine members

Subfacies H_b-I is interpreted as IHS-filled, sinuous, tidally-influenced channels, point bars, and associated overbank tidal flats occupying the middle to upper-portion of the estuarine-like funnel. Based on the conformable nature of subfacies H_b-I with the underlying facies P_{bms}, (i.e., tidally-influenced) and the sedimentary structures contained within it, a tidal origin for subfacies H_b-I is a reasonable interpretation. Although evidence for bidirectional paleoflow is rare or absent, several structures found in subfacies H_b-I meet the criteria required for differentiation of tidally-influenced river point bar deposits from wholly fluvial deposits as summarized by Thomas and others (1987):

1. Brackish cosmine-bearing fish and lingulid brachiopods are present.
2. Rhythmically interbedded couplets of sandstone, siltstone, and mudstone (i.e., FHB) constitute much of the point bar deposits.
3. Upper point bar sequences contain wave and current-ripple structures plus linsen and flaser bedding.
4. Bimodal paleoflow indicators are limited to ladderback ripples. However, sandy couplets contain an abundance of other tidal structures.
5. Some point bar sequences are characterized by intense bioturbation.

The abundance of biogenic structures (e.g., *Arenicolites* and *Skolithos*) is regarded as the single-most useful and widely applicable feature for distinguishing tidal creek point bar deposits from those of fluvial origin (Thomas and others, 1987). The low trace fossil diversity and rarity of biogenic activity in areas outside of concentrations of trace fossils suggests stressed environmental conditions related to brackish salinities and/or high concentrations of suspended sediment.

STREAKY-LAMINATED HETEROLITHIC BEDDED SUBFACIES H_B-SL

Subfacies H_b-SL occurs as two distinct units in the Sidney Mountain Quarry (outcrop 6, Fig. 5). Subfacies H_b-SL comprises a spectrum of small-scale heterolithic structures ranging from streaky-laminated sandy siltstone to sandy lenticules and wavy-bedding with discontinuous ripple cross-lamination to ripple cross-laminated fine sandstone with mud flasers (sensu Reineck and Wunderlich, 1968). Streaky-laminated sandy siltstone overlies the channel fills and the sharp, planar contact above facies P_{bms}. The streaky-lamination is characterized by pinstripe lamination as described above. Rarely, sub-millimeter thick lenses of fine sand and sandy-silt drapes are arranged as small-scale climbing oscillatory ripples similar to those described by Kvale and Archer (1991). Similar laminations have been described by Abbott (1998), Mutti and others (1985) and Homewood and Allen (1981).

No invertebrates have been identified in subfacies H_b-SL. However, concentrations of carbonized plant debris and tree bark are strewn on top bedding surfaces of sandstone lenses in the lowermost 2 meters of the unit. Trace fossils are restricted to locally abundant, short, vertical burrows resembling *Skolithos* and epichnial sinuous trails of *Planolites*.

A combined shallow marine setting of alternating storm-dominated and tidally-influenced conditions appears to be a reasonable origin for subfacies H_b-SL. Fine-grained prodelta sediments prograded in advance of sandier, tide-influenced deltaic sediments, which likely were affected by landward-directed storm currents, bidirectional (ebb-dominated) tidal currents, and possibly seaward-directed river currents during flood events. Several subaerial features prominent in tidal-flat and estuarine facies models are missing from subfacies H_b-SL. Bedding and sedimentary structures are more consistent with deposition in a shallow marine, inner-shelf, pro-delta setting. Similar deposits described by Homewood and Allen (1981) were interpreted as representing periods of alternating strong and slack currents. Homewood and Allen (1981) also suggested that millimeter- to decimeter-scale alternations in bedding thickness in facies such as subfacies H_b-SL can result from fluctuations of wave base caused by spring-neap tidal cyclicity. Alternatively, heterolithic beds such as flaser bedding and wavy-bedded sheet sandstones (i.e., middle portion of subfacies H_b-SL) may be produced solely by storms alternating with quiescent periods (McCave, 1970).

Catskill Magnafacies - Paleosols

Introduction

Five types of paleosols have been recognized in the study area. These paleosols overlie the unnamed formation of the Cattaraugus Magnafacies (i.e., caps both facies P_{bms} and H_b). A total of 7 paleosol horizons have been identified in the study area at outcrops 6 (2 horizons), 43, 51, and 53 (3 horizons) (See Figs. 4, 5). Suspected pedogenically-influenced horizons occur at outcrops 24, 34, 35, and 47. Descriptions and interpretations of these paleosols are presented below. A more complete treatment of this topic is forthcoming by Bishuk, Hairabedian and Ebert (in preparation).

Classification of Paleosols

In an attempt to provide a non-genetic, descriptive account of the paleosols, primary classification will follow the scheme proposed by Mack and others (1993). Secondary names will be assigned using the Duchaufour (1982) classification since it focuses on pedogenic process rather than modern soil properties and recognizes intergradations between classes of paleosols. Tertiary names are assigned to each paleosol in accordance with Retallack (1983) and Soil Survey Staff (1996). Interpreted names of Sonyea paleosols are summarized in Table 1.

Table 1: Classification of paleosols in outcrops of the Sonyea Group according to various systems.

OUTCROP NUMBER	PALEOSOL SYMBOL	LOCATION	Mack, James, and Monger Classification (1993)	Duchaufour Classification (1982)	Retallack Classification (1983)	Soil Survey Staff Modern Soil Classification (1996)
6	P_{gp}	Sidney Mountain Quarry, Delaware County Route 4, Sidney	Gleyed Protosol	Slightly Developed Soil	Gleyed Inceptisol	Aquic Inceptisol
6	P_{aa}	Sidney Mountain Quarry, Delaware County Route 4, Sidney	Albic Argillisol	No direct equivalent	Albic Argillaceous Inceptisol	Eutrochrept Inceptisol
43	P_{ao}	Skytop Lane Quarry, Skytop Lane, Sidney Center	Plinthite-Bearing Argillic Oxisol	Plinthite-Bearing Ferruginous Soil	Plinthite-Bearing Argillic Oxisol	Plinthic Acrustox Oxisol
43	P_{bo}	Skytop Lane Quarry, Skytop Lane, Sidney Center	Brecciated Oxisol Hardpan	Brecciated Ferruginous Soil	Brecciated Oxisol Hardpan	Lithic Acrustox Oxisol
43	P_{p}	Skytop Lane Quarry, Skytop Lane, Sidney Center	Caliche-bearing Protosol	Slightly Developed Soil	Caliche-bearing Entisol	Caliche-bearing Entisol
50*	P_{aa}	Unnamed Quarry, Intersection of Olmstead Road and Wilcox Road, East Masonville	Albic Argillisol	No direct equivalent	Argillaceous Inceptisol	Eutrochrept Inceptisol
51	P_{gp}	Sheetz Quarry, Cummings Road, East Masonville	Gleyed Protosol	Slightly Developed Soil	Gleyed Inceptisol	Aquic Inceptisol
53	P_{gp}	Delaware County Route 27, Sidney Center	Gleyed Protosol	Slightly Developed Soil	Gleyed Inceptisol	Aquic Inceptisol
53	P_{aa}	Delaware County Route 27, Sidney Center	Albic Argillisol	No direct equivalent	Albic Argillaceous Inceptisol	Eutrochrept Inceptisol

NOTES:
* = More research is necessary at this outcrop for positive identification of paleosol; Paleosol names provided are preliminary.

Non-Brecciated Argillic Oxisol and Related Units – Paleosols P_{ao}, P_{bo}, and P_p and Facies CF_{ss} at Outcrop 43, Skytop Lane Quarry, Sidney Center

Many of the paleosols described in Table 1 can be studied at a single outcrop near Sidney Center – the Skytop Lane Quarry (outcrop 43; Figs. 5, 7). Channels that incise paleosols are present as are lateral changes in paleosol type. This outcrop will be the centerpiece of the field trip.

Channel Form Silty Sandstone Facies (CF_{ss})

Facies CF_{ss} occurs as laterally discontinuous, concave-upward channel forms measuring up to 10 meters wide, which incise up to 0.5 meters into paleosol P_{ao}. Two channels of CF_{ss} are present at outcrop 43 (Fig. 7). Alternating beds of siltstone and silty, very fine sandstone fill the channels. Trough crossbeds with dip angles averaging 30-35 degrees are the dominant sedimentary structure within the center of the channels. These crossbeds are commonly contorted by soft sediment deformation. Near the edges of the channels, low-angle laminations generally approximate the concave-upward shape of the channel. Edges of channels pinch out to approximately 10-15 cm thick and grades into horizons A_k/A_{ao} of paleosol P_{ao}. No body fossils, trace fossils, or evidence of pedogenesis occur in facies CF_{ss}.

Facies CF_{ss} represents ephemeral wash channels incised into the paleosols of stable interfluves in a semi-arid environment. Soft sediment deformation in the channels suggests rapid deposition during floods. There is no evidence of tidal-influence in facies CF_{ss}. The geometry of facies CF_{ss} indicates these wash channels were stable in position for a prolonged period of time. Lateral bank erosion was probably inhibited or completely halted by the resistant nature of parts of the adjacent paleosols. Downcutting of these channels was hampered by low seasonal discharge and the erosional resistance of the paleosols. These ephemeral wash channels offer insight into the nature of the paleocoastal landscape at a major unconformable surface. They also provide evidence that river avulsion caused a drastic decrease in discharge to the paleocoastline, which set up prolonged conditions for the development of paleosols in the interfluves (Boswell and Donaldson, 1988).

Paleosol (P_{ao})

A moderately well developed, non-brecciated, argillic oxisol (paleosol P_{ao}) caps facies H_b at outcrop 43 (Fig. 9). Paleosol P_{ao} gradationally overlies facies H_b and is sharply overlain by facies T_{xb}-ti. The contact of paleosol P_{ao} and facies T_{xb} is predominantly non-erosional, preserving underlying delicate pedogenic features, but is erosional locally with channels incised up to 0.5-1 meter into the paleosol. Rarely, the channel-form silty sandstone facies (facies CF_{ss}) occurs between paleosol P_{ao} and facies T_{xb}.

Paleosol P_{ao} ranges in thickness from 75 cm to 95 cm. Four pedogenic horizons exist - a laminar calcrete crust (A_k), a plinthite-bearing melanic epipedon (A_{ao}), an argillic horizon (B_t), and a nodule-bearing horizon with vestigial bedding (C_c). Paleosol P_{ao} can be traced laterally approximately 100 meters across outcrop 43, but appears to change character into another type of paleosol (paleosol P_p) to the northeast across the remaining 200-300 meters of the outcrop.

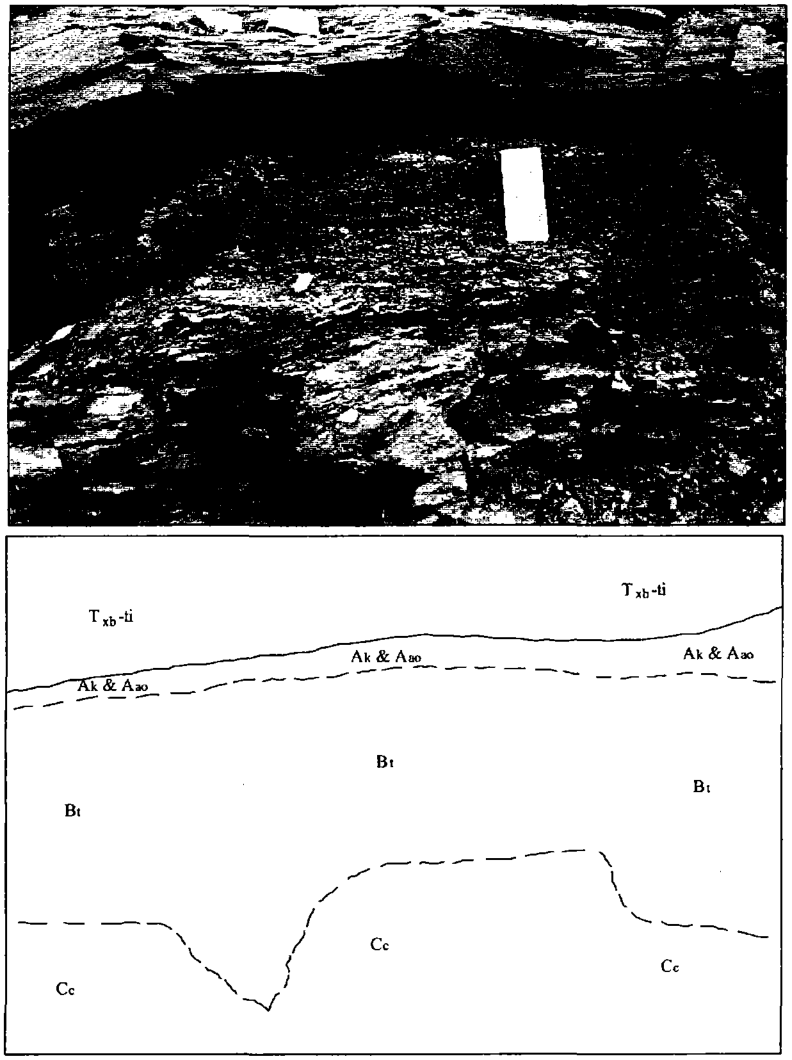

Fig. 9 Field photo and tracing argillic oxisol (paleosol P_{ao}) horizonation. Paleosol is abruptly overlain by the tidally-influenced trough cross-bedded facies (outcrop 43).

<u>A_k Horizon – Laminar Calcareous Crust</u>

The A_k horizon is a continuous, 1-5 mm thick, structureless, white to light gray crust (Munsell colors = GLEY1 8/N) that blankets the A_a horizon, similar to that described by Lattman (1973). The crust is powdery and weakly calcareous. This crust is laterally continuous for a minimum of 20 meters, extending to the edge of the outcrop. Locally, crude microlaminations are discernable. Reaction to hydrochloric acid is weak to moderate. In some places, the layer is replaced laterally by light gray (5Y 7/2), highly plastic, calcareous clay.

A_{ao} Horizon – Plinthite-Bearing Melanized Epipedon

The A_{ao} horizon is a dark gray/black to dark reddish gray hardpan cemented by amorphous iron oxide with localized zones of a humus-poor, iron and organic matter complex, which qualifies it as a plinthite (formerly known laterite) layer (Retallack, 2001). Bitumen is abundant on the top surface of the hardpan as well as sparse unidentifiable plants (i.e., humus-poor zone). The hardpan ranges in thickness from 5-10 mm and is laterally continuous for at least 25 meters to the edge of the outcrop. The hardpan is always associated with the A_k horizon.

The basal portion of the A_{ao} horizon ranges in thickness from 4 to 10 cm. It is characterized by a distinct darkening (GLEY2 3/5 – dark bluish gray) caused by the accumulation of abundant organic matter (bitumen and sparse unidentifiable plant remains) with lesser concentrations of amorphous iron oxide. Numerous glaebules occur in the form of sesquioxidic, ferruginous nodules, consisting of amorphous iron oxide. The ferruginous nodules show an increase in size upward from the base of A_{ao} to the base of the overlying plinthite. These elliptical nodules are so abundant that they form a peppered fabric throughout the thin sections. The nodules commonly disrupt microlaminae and also occur as thin coatings of amorphous iron oxide on microlaminae. The darkest layers of iron oxide anastomose and bifurcate. In the field, the degree of mottling is 30-40 %, with subordinate colors ranging from light gray (5Y 7/2), yellowish brown (10YR 5/6), and pale olive (5Y 6/3). Concentrations of plant stems and leaf fronds occur as a mat-like fabric, which resembles sparse leaf litter.

Crude vestigial laminations of alternating silty, very fine sandstone and medium to coarse sandstone lenses are present. Micro-scale planar laminations and current ripple cross-laminations are readily seen with the naked eye on thin section mounts. The A_{ao} horizon grades laterally into silty sandstone beds of facies CF_{ss}, thereby establishing a close genetic association between A_{ao} and CF_{ss}. The original bedding is overprinted by a platy ped fabric. Concentrations of bitumen commonly coat the parting surfaces of peds. No accumulation of clay was observed in the A_{ao} horizon.

B_t Horizon – Argillic Horizon

The B_t horizon is characterized by subangular to angular blocky peds composed of siltstone and very fine sandy siltstone. The dominant colors in the B_t horizon are light greenish gray (GLEY1 8/10Y) and white (GLEY1 8/N). Degree of color mottling is 20-25%, with subordinate colors ranging from reddish brown (5YR 5/8 and 5YR 6/8) and dark bluish gray (GLEY2 3/5PB). The B_t horizon thickness ranges from approximately 50 to 90 cm and is laterally continuous for approximately 100 meters. Ped structures are commonly infilled with clay argillans and coated with quasiferrans (i.e., two forms of illuviation cutans). The composition of these illuviation cutans is likely illite swelling clay and cryptocrystalline hematite or goethite, respectively. Concentrations of clay argillan material are greatest at the top of the B_t horizon and decreases downward. Locally, clay argillans are absent and ped surfaces are stained by sesquioxidic quasiferrans. Pedogenic slickensides (i.e., stress cutans) are rare, but locally occur in the mid- to lower-portion of the B_t horizon. Glaebules occur in the form of small goethite concretions and homogeneous caliche nodules measuring 0.2-2 cm in diameter, but are relatively uncommon. Roots, rhizoliths, rhizocretions, and pedotubules are absent. Rare lenses of an amorphous iron oxide and darkened organic matter complex, similar in composition and appearance to the A_{ao}

horizon, occur within the uppermost 10 cm of the B_t horizon. These lenses measure 3-5 cm thick and up to approximately 50 cm long.

C_c Horizon – Nodular-Bearing Horizon with Vestigial Bedding

The C_c horizon is characterized by vestigial heterolithic bedding of facies H_b. Pedogenic features are restricted to glaebules, which occur in the form of small (0.2-3 cm, but average <1 cm) caliche nodules. These nodules are rare, but tend to occur in clusters (i.e., possible rhizocretion accumulations). No roots, rhizoliths, rhizocretions, or pedotubules were observed. *Skolithos* and *Arenicolites* burrows and *in loco* plant fragments are exceedingly common in vestigial fine sandstone interbeds.

Paleosol P_{ao} is interpreted as a moderately-well developed argillic oxisol (Table 1). Pedogenic features present in paleosol P_{ao} make a strong case that processes such as hydrolysis, hydration, dissolution, oxidation, leaching, and acidification were either intense, prolonged, or both. The advanced weathering of the oxisol profile is an indicator of great age, which can amount to tens of millions of years (Retallack, 2001). However, a more realistic estimate of the oxisol age is 20-400 thousand years, which is based on rates of modern hardpan development (Williams and Krause, 2000).

OTHER PALEOSOLS AT OUTCROP 43 – PALEOSOL P_{BO} AND PALEOSOL P_P

A brecciated oxisol (paleosol P_{bo}) (Fig. 10) and protosol (paleosol P_p) are found interdigitated with paleosol P_{ao} in the Skytop Lane Quarry. Paleosols P_{bo} and P_p gradationally overlie facies H_b-ti and are sharply overlain by facies T_{xb}. Paleosols P_{bo} and P_p are generally 1 meter or less in thickness. Three pedogenic horizons exist in paleosol P_{bo}, including a sesquioxic-nodular, brecciated horizon (B_{co}) with evidence of early lithification, an argillic horizon (B_t), and a horizon which bears caliche nodules and vestigial bedding (C_c), which are remnants of heterolithic bedding in facies H_b. Lateral continuity of discontinuous sections of paleosol P_{bo} is poor across outcrop 43, ranging from 5-25 meters.

Fig. 10 Brecciated oxisol (paleosol P_{bo}) at STOP #1. See Figs. 4 and 7 for position of this paleosol. DNAG card on the paleosol provides scale.

Paleosol P_{bo} is interpreted as a moderately-well developed brecciated oxisol hardpan (Table 1). Degree of pedogenesis in paleosol P_{bo} is mild to moderate as compared to features present in paleosol P_{ao}. The presence of numerous sub-rounded clasts of variable lithology (i.e., weathered calcrete, siltstone, and shale) indicates that some material was transported rather than *in situ* parent material. The laterally adjacent position of paleosol P_{bo} in relation to facies CF_{ss} is significant. It may indicate that paleosol P_{bo} is a pedogenically-altered remnant of a point bar of the ephemeral wash channels of facies CF_{ss}

No horizonation is discernable in paleosol P_p. It contains only a nodular-bearing horizon with vestigial bedding (C_c). Paleosol P_p is interpreted as a protosol, which was subjected to minor levels of pedogenesis. Similar to the C_c horizon of paleosol P_{ao}, pedogenesis is restricted to caliche nodules (i.e., glaebules). Paleosol P_p is laterally proximal to a large channel form infilled with tidally-influenced sedimentary structures. It appears likely that frequent tidal flooding diminished or disrupted pedogenesis.

Albic Argillisol– Paleosol P_{aa}

A moderately developed, albic argillisol (paleosol P_{aa}) underlies facies T_{xb}-ti at outcrop 53 in Sidney Center, and caps facies P_{bms} at outcrop 6 (Sidney Mountain Quarry- STOP 3; Fig. 5). At outcrop 6, paleosol P_{aa} sharply overlies facies P_{bms}. A second occurrence of paleosol P_{aa} at outcrop 6 is sharply overlain by marine deposits of facies S_{dg} and H_{cs}. The contact of paleosol P_{aa} and facies P_{bms} is minimally-erosional, preserving underlying E horizon features, but is locally erosional with channels incised up to 0.5-1 meter into the paleosol. The contact of paleosol P_{aa} and facies S_{dg} and H_{cs}, occurring at the top of outcrop 6, appears to be minimally-

erosional as well, with localized relief up to 1 meter at the contact on an otherwise sharp and planar contact.

Paleosol P_{aa} ranges in thickness from 1.7 meters at outcrop 6 to 4.5 meters at outcrop 53. Pedogenic horizonation is weak. Recognized horizons include a leached albic horizon (E), an argillic horizon (B_t), and a rooted sandstone horizon (C). Paleosol P_{aa} laterally replaces paleosol P_{gp} at outcrop 6, and occurs twice (i.e., 18-19.5 m and 22-24.5 m on Fig. 5). P_{aa} is distinguished from P_{gp} by the absence of relict bedding.

Paleosol P_{aa} supported mono-specific stands of plants further away from coastal waterways in comparison to paleosol P_{gp}, but was still influenced by infrequent flooding from them (i.e., likely 100-year and 500-year flood events). This is in marked contrast to paleosols P_{ao}, P_{bo}, and P_p, which is best explained by differences in relative distances from active paleochannels.

Since the E horizon is directly overlain by marine deposits of facies P_{bms} at outcrop 6 and facies $T_{xb\text{-}ti}$ at outcrop 53, it is possible that overprinting of pedogenic patterns by early marine physical and chemical processes (i.e., marine hydromorphism) occurred at these locations (Fig. 11). This occurrence bears similarities to features described by Driese, Mora, and Cotter (1993). Chemical analysis or X-ray diffraction is necessary to confirm the presence or absence of chemical signatures of marine hydromorphism in paleosol P_{aa}.

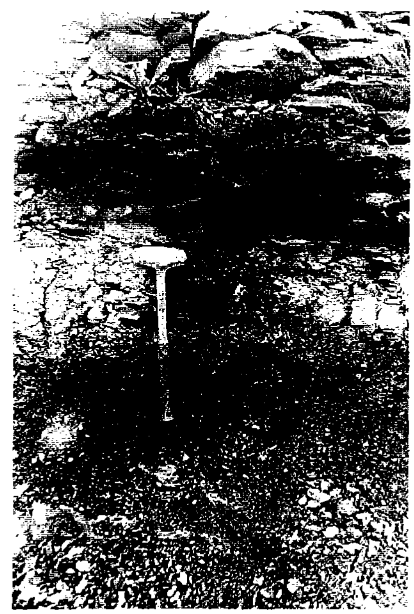

Fig. 11 Possible marine hydromorphism of paleosol at outcrop 53. Paleosol is overlain by marine sediments of the planar-bedded multistorey sandstone facies

Gleyed Protosol– Paleosol P_{gp}

A poorly developed, gleyed protosol (paleosol P_{gp}) caps facies P_{bms} at outcrop 51 (Sheetz Quarry- STOP 2), outcrop 6 (Sidney Mountain Quarry- STOP 3), and outcrop 53. Paleosol P_{gp} sharply overlies facies P_{bms} and contains vestigial heterolithic bedding from facies H_b. Paleosol P_{gp} is sharply overlain by facies P_{bms} or sharply overlain by marine facies S_{dg} and H_{cs}. The contact of paleosol P_{gp} and facies P_{bms} is minimally-erosional, preserving underlying E horizon features, but is locally erosional with a channel incised up to 0.5-1 meter into the paleosol.

Paleosol P_{gp} ranges in thickness from 0.4 meters at outcrop 53 to 1.7 meters at outcrop 6. Paleosol P_{gp} can be traced to the lateral extents of each outcrop; several hundred meters at outcrops 6 and 51 and less than 50 meters at outcrop 53. At outcrop 6, paleosol P_{ap} occurs interdigitated with paleosol P_{gp}. Pedogenic horizonation is poor; therefore abundant primary sedimentary structures are preserved. Recognized horizons are limited to a leached albic horizon (E) and a pedogenically-influenced, vestigially bedded horizon (C_c). An abrupt horizon of red-green mottling occurs at the contact of vestigial heterolithic bedding with facies P_{bms}, and generally decreases in intensity upward in paleosol P_{gp}. Ped fabrics are very weak to absent, exhibiting a cryptic platy framework. The most common features at outcrops 51 and 53 are drab root haloes, which consists of 0.5-5 mm diameter rhizoliths (i.e., filled and unfilled varieties) with boundaries of bluish gray to greenish gray haloes extending out into the paleosol matrix (See also Retallack, 2001). Mat-like rhizomatous networks occur in mudrocks between successive sandstone beds within vestigial heterolithic bedding. One possible ornamental leaf-like structure with associated node-like basal attachment, tentatively identified as *Drapanophycus*, has been collected from these horizons (Fig. 12). Rarely, large diameter tap roots measuring up to 0.5-1 cm are found, as are rare caliche nodules.

Fig. 12 Leaf-like structure tentatively identified as *Drapanophycus.*

The color mottling exhibited by this paleosol is a diagnostic feature of waterlogged soils and is a conspicuous feature of groundwater gley (Retallack, 1997). Mottling is also characteristic of frequent exposure to redox fluctuations (Driese and others, 1997). Based on the shallow, dominantly horizontal, mat-like fabric of root traces, P_{gp} is considered the product of groundwater gley associated with a shallow groundwater table along coastal waterways.

Paleosol P_{gp} is interpreted as a gleyed protosol, which supported mono-specific stands of flood-resistant plants on the banks of fresh-water channels on the distal alluvial plain at outcrop 51 and tidally-influenced deltaic channels at outcrops 6, 53 and possibly 51. Evidence for tidal-influence is clear at outcrops 6 and 53, suggesting that plant stands along the banks of delta channels and tidal flats were tolerant of brackish water conditions. The exact type of plants living in these coastal habitats is unknown, since *in situ* aerial portions of plants attached to roots are absent. However, the horizontal, mat-like rhizomatous fabric is reminiscent of fungi (i.e., calcified fungal mycelia or possibly lichen rhizomes) characterized by Driese and others (2001). Driese and others (1992) found that these fungi lived in moist, pedogenically modified deposits of coastal mudflats and marshes. Alternatively, the rhizomatous fabric is similar to the reconstruction of the root system of the early lycophyte *Drapanophycus spinaeformis* (Driese and others 2001). The presence of *in situ* lycophytes is a possibility, since *Drapanophycus*-like structures were found. The identity of plants that produced the large diameter tap roots is unknown.

FACTORS AFFECTING SONYEA PEDOGENESIS

Paleosols of the Sonyea Group developed on coastal-margin interfluves and show a wide variability that can be explained by sea level position/fluctuation, drainage characteristics of adjacent and underlying sediments, an avulsion-controlled style of coastal-margin basin filling and tectonically induced subsidence. The sequence of events leading to Sonyea paleocoastline development is summarized in Fig. 13. Based on the consistent stratigraphic position of these paleosols (Figs. 4, 5), well developed paleosols record pedogenesis during periods of reduced or negative accommodation (i.e., slight base level fall). Repetition of the following sequences of processes is interpreted to have occurred: 1) sea-level rise (transgressive system tract), 2) peak sea-level rise slows to a pause (highstand system tract), 3) river avulsions and slight lowering of sea-level (falling stage to lowstand systems tracts) with coeval pedogenesis, 4) episodic subsidence associated with epeirogenic downflexure of the lithosphere (Quinlan and Beaumont, 1984), and 5) coastal drowning associated with renewed eustatic sea-level rise. Differences in paleosol characteristics are attributable to the time allowed for pedogenesis, during both autocyclic and high order (i.e., 4^{th} and 5^{th} order) eustatic fluctuations.

Changes in the Sonyea shoreline are characterized as "mixed shift" (Boswell and Donaldson 1988), where transgression is displayed in some parts of the shoreline, and regression along others. Mixed shifting is the result of changes in the distribution or supply of sediments as controlled by autocyclic processes such as river avulsions. Boswell and Donaldson (1988) determined that major rivers had relatively fixed positions in the Famennian portions of the Catskill clastic wedge, which created large, long-lived interfluve areas where tidal processes dominated. It is clear from this investigation that similar conditions existed in the study area during Frasnian time.

Sonyea paleosols formed near coastal sandflats and mudflats. During initial stages of soil development, the water table was probably close to the surface most of the time, and reducing conditions prevailed (e.g., paleosols P_{gp}, P_{aa}, and P_p). The rate of overbank deposition of the tidally-influenced coastal waterways controlled the degree of pedogenesis. Some areas of the Sonyea coast experienced major river avulsions, starving some interfluves of sediment and creating new interfluves. Avulsion probably resulted in soils with lower water tables on newly created interfluves (i.e., paleosols P_{ao}, and P_{bo}), whereas areas that continued to receive sediment along active distal rivers remained waterlogged with high water table conditions (i.e., paleosols P_{gp}, and P_{aa}). The post-avulsion paleolandscape was probably a somewhat barren, semi-arid desert shrubland, possibly dominated by Aneurophytes, which also dominated marine bayfill/prodelta deposits and coastal-margin paleosols of the early Frasnian Oneonta Formation in the Catskill clastic wedge (Scheckler and others, 2000).

In loco plant remains of Archeopteris in paleosol P_{ao} indicates that vegetated stream banks were localized upstream in fresher water habitats, such as river courses. These fresh-water habitats must have been close to the brackish waterways. Archeopteris populations probably decreased rapidly after avulsions when reduced discharge and lower water tables caused habitat loss.

Comparison of Sonyea paleosols with other Devonian paleosols in the Appalachian Basin

Interest in coastal-margin paleosols in the Devonian Catskill clastic wedge has increased over the past decade (Driese, Mora, and Cotter, 1993a and 1993b; Cotter, Mora, Fastovsky, and Driese, 1993; Driese, Mora, and Elick, 1997; Scheckler and others, 2000; Schieber, 1999; and Driese, Mora, Cotter, and Foreman, 1992). Paleosols reported show wide variability, but there is a general consensus of a semi-arid paleocoastal environment. These variations, as well as the oxisols and argillisols reported in this study, are consistent with a semi-arid paleoclimate. The coastal-margin gleysols and protosols reported by Cotter and others (1993) and Driese and others (1997) appear to be the closest matches to paleosols P_{gp}, P_{aa}, and P_p. Paleosols similar to P_{ao} and P_{bo} have not been reported in other portions of the Catskill clastic wedge.

Conclusions

Portions of the Frasnian Sonyea Group in northwestern Delaware County are comprised of the Cattaraugus Magnafacies, which represents nearshore and shoreline environments in the Catskill clastic wedge. These facies record a mosaic of tidally-influenced subenvironments in an overall estuarine setting. Facies that record tidally-influenced marginal marine environments succeed one another laterally and vertically and are complexly interleaved with fully marine facies and terrestrial paleosols. In many locations, paleosols developed directly on tidally-influenced facies and are overlain by facies of obvious marine or marginal marine origin. These stratigraphic relationships indicate a "mixed shift" shoreline in which progradation and retrogradation could be contemporaneous in adjacent areas. Avulsion and sediment supply were primary controls on which segments of the Sonyea shoreline prograded or retrograded during the overall Frasnian transgression. Episodes of tectonically induced subsidence and pulses of eustatic rise accelerated onlap, especially in areas from which sediment supply was diverted by avulsion. The newly recognized paleosols in the Sonyea Group have proven to be critical clues to understanding the dynamics of the Catskill shoreline.

Several types of paleosols developed on Sonyea coastal-margin interfluves under a semi-arid climatic regime. The formation of individual paleosols was terminated by marine inundation produced by decreased sediment supply via avulsion and/or high order eustatic fluctuations. Therefore, differences in paleosol characteristics resulted from differing durations of pedogenesis before inundation. The relative position of the water table and proximity to brackish channels were also important factors influencing the development of Sonyea paleosols. Some paleosols were vegetated, but it is likely that the flora was restricted to areas adjacent to channels where the water table was high. Paleosols with limited degrees of pedogenesis (e.g., gleysols and protosols) have been reported from similar paleoenvironments elsewhere in the Catskill clastic wedge. However, paleosols with greater degrees of pedogenesis such as the oxisols and argillisols in the Sonyea Group have not been reported elsewhere. These more advanced stages of pedogenesis may indicate a subtle increase in the aridity of the climate in the Late Devonian.

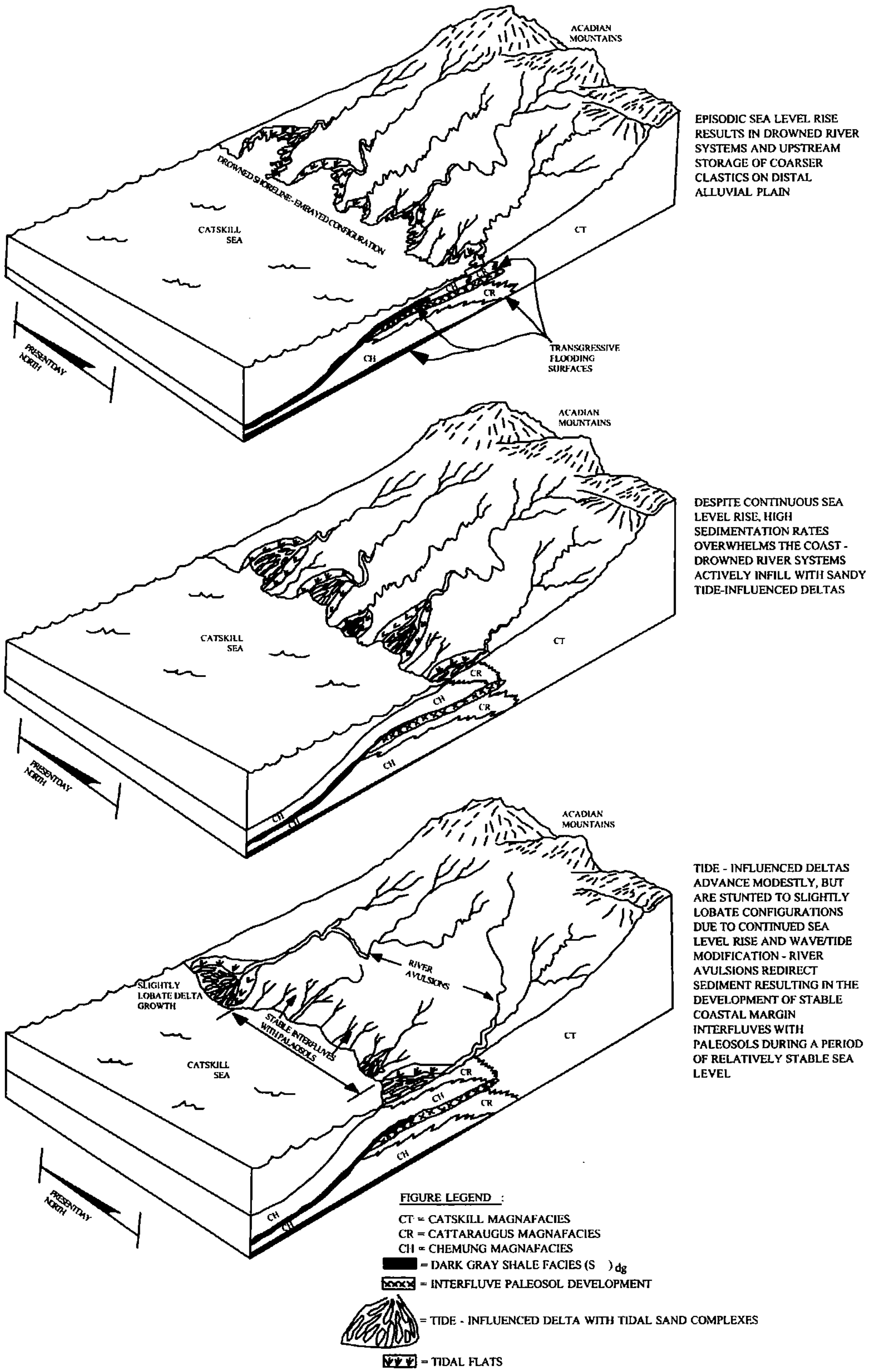

Fig. 13 Schematic, three-dimensional reconstruction of sedimentary environments and progressive development of shoreline configuration and depositional cyclicity. Note the intimate association of paleosols with fully marine and tidally-influenced paleoenvironments.

ACKNOWLEDGEMENTS

This paper constitutes a major expansion upon parts of the M.A. thesis of D. Bishuk, completed at SUNY Oneonta. We thank Dr. Edward Cotter for helpful field discussions at several outcrops and follow-up correspondence during early versions of the manuscript, which helped refine our facies and paleosol interpretations. We are greatly indebted to Sherri Pullar of EA Science and Technology for her outstanding AutoCad drafting services. This project would not have reached its current level of completeness without the undergraduate research contributions of Ann McSpedon, which consisted of thin section preparation and analysis, and preliminary interpretations of paleosol micromorphology. Much love and appreciation is extended to Mary Bishuk for enduring support and understanding over the 3-year research period.

REFERENCES CITED

Abbott, Stephen T., 1998, Transgressive systems tracts and onlap shellbeds from Mid-Pleistocene sequences, Wanganui Basin, New Zealand: Journal of Sedimentary Research, v. 68, no. 2, p. 253-268.

Barrel, J., 1913, The Upper Devonian delta of the Appalachian geosyncline: American Journal Science, 4th ser., v. 36, p. 429-472.

Barrel, J., 1914, The Upper Devonian delta of the Appalachian geosyncline: American Journal Science, 4th ser., v. 37, p. 87-109.

Bishuk, Jr., Daniel, 1989, Nondeltaic Marginal-marine Processes and Products in the Catskill Clastic Wedge, Upper Devonian Sonyea Group, South-Central New York. Unpublished M.A. Thesis. State University of New York at Oneonta.

Bishuk, Jr., D., Applebaum, R., and Ebert, J.R. 1991, Storm-dominated shelf and tidally-influenced foreshore sedimentation, Upper Devonian Sonyea Group, Bainbridge to Sidney Center, New York: New York State Geological Association, 63rd Annual Meeting, Oneonta, Field Trip Guidebook, p. 413-462.

Bishuk, Jr., D., Hairabedian, J., and Ebert, J.R., (in preparation for 2004), Forthcoming article in the Journal of Sedimentary Research.

Blieck, A., 1982, Donnees nouvelles sur les Heterostraces (Vertevres, Agnathes) du gisement d'Ombret, Devonien inferieur de l'Ardenne belge: Ann. Soc. Geol. Belg., v. 105, no. 2, p. 235-239.

Blieck, A., 1985, Paleoenvironnements des Heterostraces, Vertebres agnathes ordov iciens a devoniens: In Fischer, J.C. (organ.), Journees d'etude sur les indicateurs paleobiologiques de milieux (RCP 641, Paris, 26-27 mars 1984), Bull. Mus. Natn. Hist. Nat., 4e ser., v. 7, no. 2, p. 143-155.

Boswell, R.M, and Donaldson, A.C., 1988, Depositional architecture of the Upper Devonian Catskill Delta complex: Central Appalachian basin, U.S.A.: In McMillan, N.J., Embry, A.F. and Glass, D.J. (eds.), Devonian Of The World, Volume II: Sedimentation, Canadian Society of Petroleum Geologists, p. 65-84.

Bridge, John S., Gordon, Elizabeth A., and Titus, Robert C., 1986, Non-marine bivalves and associated burrows in the Catskill Magnafacies (Upper Devonian) of New York State: Paleogeography, Paleoclimatology, and Paleoecology, v. 55, p. 65-77.

Bridge, John S., 2000, The geometry, flow patterns and sedimentary processes of Devonian rivers and coasts, New York and Pennsylvania, USA: In Friend, P.F., and Williams, B.P.J., (eds.), New perspectives on the Old Red Sandstone, Geological Society of London, Special Publications 180, p. 61-84.

Bridge, John S., and Droser, Mary L., 1985, Unusual marginal-marine lithofacies from the Upper Devonian Catskill clastic wedge: In D.L. Woodrow and W.D. Sevon (eds.), The Catskill Delta, Geological Society of America special paper 201, p. 163-181.

Bridge, John S., and Willis, B.J., 1994, Marine transgressions and regressions recorded in Middle Devonian shore-zone deposits of the Catskill clastic wedge: Geological Society of America Bulletin, v. 106, p. 1440-1458.

Coleman, J.M., Gagliano, S.M., and Webb, J.E., 1964, Minor sedimentary structures in a prograding distributary: Marine Geology, v. 1, p. 240-258.

Cotter, E., Mora, C., Fastovsky, D., and Driese, S., 1993, Paleosols in Irish Valley and Sherman Creek Members of Catskill Formation Near Selinsgrove, Pennsylvania: In Driese, Steven G., Mora, C.I., and Cotter, E., (eds.), Paleosols, paleoclimate, and paleoatmospheric CO_2: Paleozoic paleosols of central Pennsylvania: University of Tennessee, Department of Geological Sciences, Studies in Geology, no. 22, p. 66-75.

Craft, J.H. and Bridge, J.S., 1987, Shallow-marine sedimentary processes in the Late Devonian Catskill Sea, New York State: GSA Bulletin, v. 98, p. 338-355

Davies, G.R., 1977, Turbidites, debris sheets, and truncation surfaces in Upper Paleozoic deep water carbonates of the Sverdrup Basin, Artic Archepelago: In Cook, H.E., and Enos, P. (eds.), Deep-water carbonate environments, SEPM Special Publication no. 25, p. 221-247.

Dalrymple, R.W., Zaitlin, B.A., and Boyd, R., 1992, Perspective: Estuarine facies models: Conceptual basis and stratigraphic implications: Journal of Sedimentary Petrology, v. 62, no. 6, p. 1130-1146.

De Mowbray, T., and Visser, M.J., 1984, Reactivation surfaces in subtidal channel deposits, Oosterschelde, Southwest Netherlands: Journal of Sedimentary Petrology, v. 54, no. 3, p. 811-824.

Driese, Steven G., and Cotter, E., 1997, Paleosol changes along a coastal-margin to alluvial-plain transect: Catskill Fm. (Upper Devonian), Central Pennsylvania: GSA Annual Meeting, Salt Lake City, v. ??, no. ??, p. A-431-A-432.

Driese, Steven G., Mora, C.I., and Cotter, E., 1993, Paleosols, paleoclimate, and paleoatmospheric CO_2: Paleozoic paleosols of central Pennsylvania: University of Tennessee, Department of Geological Sciences, Studies in Geology, no. 22, 136 p.

Driese, Steven G., Mora, C.I., and Elick, J.M., 1997, Morphology and taphonomy of root and stump casts of the earliest trees (Middle to Late Devonian), Pennsylvania and New York, U.S.A.: Palaios, v. 12, p. 524-537.

Driese, Steven G., and Mora, C.I., 2001, Diversification of Siluro-Devonian plant traces in paleosols and influence on estimates of paleoatmospheric CO_2 level: In Gensel, Patricia G., and Edwards, Dianne (eds.), Plants invade the land: Evolutionary and environmental perspectives, Columbia University Press, New York, p. 237-253.

Driese, Steven G., and Mora, C.I., Cotter, E., and Foreman, J.L., 1992, Paleopedology and stable isotope chemistry of Late Silurian vertic paleosols, Bloomsburg Formation, Central Pennsylvania: Journal of Sedimentary Petrology, v. 62, no. 5, p. 825-841.

Duchaufour, P., 1982, Pedology, Allen and Unwin, London, England, 448 p.

Fenies, H., and Tastet, J.P., 1998, Facies and architecture of an estuarine tidal bar (the Trompeloup bar, Gironde Estuary, SW France): Marine Geology, v. 150, p. 149-169.

Friedman, Gerald M., and Chamberlain, John A., 1995, Archanodon Catskillensis (Vanuxem): Fresh-water clams from one of the oldest back-swamp fluvial facies (Upper Middle Devonian), Catskill Mountains, New York: Northeastern Geology and Environmental Sciences, v. 17, no. 4, p. 431-443.

Gordon, Elizabeth A., 1988, Body and trace fossils from the Middle-Upper Devonian Catskill Magnafacies, Southeastern New York, U.S.A.: In McMillan, N.J., Embry, A.F., and Glass, D.J. (eds.), Devonian of the world: Volume II: Sedimentation, Proceedings of the second international symposium on the Devonian system, Canadian Society of Petroleum Geologists, Calgary, Alberta, Canada, p. 139-156.

Griffing, D.H., Bridge, J.S., and Hutton, C.L., 2000, Coastal-fluvial palaeoenvironments and plant palaeoecology of the Lower Devonian (Emsian), Gaspe Bay, Quebec, Canada: In P.F. Friend and B.P.J. Williams (eds.), New perspectives on the Old Red Sandstone, Geological Society of London special publication no. 180, p. 61-84.

Halperin, A., and Bridge, J.S., 1988, Marine to non-marine transitional deposits in the Frasnian Catskill clastic wedge, south-central New York: In McMillan, N.J., Embry, A.F. and Glass, D.J. (eds.), Devonian Of The World, Volume II: Sedimentation, Canadian Society of Petroleum Geologists, p. 107-124.

Hamblin, A.P., and Walker, R.G., 1979, Storm-dominated shallow marine deposits: The Fernie-Kootenay (Jurassic) transition, southern Rocky Mountains: Canadian Journal of Earth Science, v. 16, p. 1673-1690.

Harms, J.C., Southard, J.B., Spearing, D.R., and Walker, R.G., 1975, Depositional environments as interpreted from primary sedimentary structures and stratification sequences: Society of Economic Paleontologists and Minerologists Short Course No. 2, Dallas, Texas, 161 p.

Homewood, P., and Allen, P.A., 1981, Wave-, tide- and current-controlled sandbodies of Miocene Molasse, western Switzerland: Bulletin of the American Association of Petroleum Geologists, v. 65, p. 2534-2545.

Johnson, K.G., and Friedman, G.M., 1969, The Tully clastic correlatives (Upper Devonian) of New York State: A model for recognition of alluvial dune(?), tidal, nearshore (bar and lagoon), and off-shore sedimentary environments in a tectonic delta complex: Journal of Sedimentary Petrology, v. 39, p. 451-485.

Johnson, J.G., Klapper, G., and Sandberg, C.A., 1985, Devonian eustatic fluctuations in Euramerica: GSA Bulletin, v. 96, p. 567-587.

Kirchgasser, W.T., Over, D.J., and Woodrow, D.L., 1994, Frasnian (Upper Devonian) Strata of the Genesee River Valley, Western New York State, In Brett, Carlton E. and Scatterday, James (eds.), Field trip guidebook, New York State Geological Association, 66th Annual Meeting, p. 325-358.

Kraus, M.J., 2000, Paleosols in clastic sedimentary rocks: their geologic applications, Earth Science Reviews, v. 47, p. 41-70.

Kvale, E.P., and Archer, A.W., 1991, Characteristics of two, Pennsylvanian-aged semidiurnal tidal deposits in the Illinois Basin, U.S.A.: In Smith, D.G., Reinson, G.E., Zaitlin, B.A., and Rahmani, R.A., Clastic tidal sedimentology, Canadian Society of Petroleum Geologists Memoir 16, Calgary, Alberta, p. 179-188.

Lattman, L.H., 1973, Calcium carbonate cementation of alluvial fans in southern Nevada: Geological Society of America Bulletin, v. 84, p. 3013-3028.

Linsley, David M., 1994, Devonian Paleontology of New York: Paleontological Research Institution, Special Publication no. 21, 472 p.

Mack, Greg H., James, W.C., and Monger, H.C., 1993, Classification of paleosols: Geological Society of America Bulletin, v. 105, p. 129-136.

Marzo, M., and Steel, R.J., 2000, Unusual features of sediment supply-dominated, trangressive-regressive sequences: Paleogene clastic wedges, SE Pyrenean foreland basin, Spain: Sedimentary Geology, v. 138, p. 3-15.

McCave, I.N., 1970, Deposition of fine-grained suspended sediment from tidal currents: Journal of Geophysical Research, v. 75, p. 4151-4159.

McCrory, V.L., and Walker, R.G., 1986, A storm and tidally-influenced prograding shoreline: Upper Cretaceous Milk River Formation of Southern Alberta, Canada: Sedimentology, v. 33, no. 1, p. 47-60.

Miller, M.F., 1979, Paleoenvironmental distribution of trace fossils in the Catskill delta complex, New York State: Palaeogeography, Palaeoclimatology, and Palaeoecology, v. 28, p. 117-141.

Mutti, E., Rosell, J., Allen, G.P., Fonnesu, F., and Sgavetti, M., 1985, The Eocene Baronia tide-dominated delta-shelf system in the Ager Basin: 6th European Regional Meeting Excursion Guidebook, International Association of Sedimentologists, University of Barcelona, Spain, p. 579-600.

Nio, S.D., and Yang, C.S., 1991, Diagnostic attributes of clastic tidal deposits: A review: In Smith, D.G., Reinson, G.E., Zaitlin, B.A., and Rahmani, R.A. (eds.), Clastic tidal sedimentology, Canadian Society of Petroleum Geologists Memoir 16, Calgary, Alberta, p. 3-28.

Okazaki, H., Masuda, F., 1995, Sequence stratigraphy of the late Pleistocene Palaeo-Tokyo Bay: barrier islands and associated tidal delta and inlet: Special Publications of the International Association of Sedimentologists, No. 24, p. 275-288.

Quinlan, G.M., and Beaumont, C., 1984, Appalachian thrusting and the Paleozoic stratigraphy of the eastern interior of North America: Canadian Journal of Earth Science, v. 21, p. 973-994.

Retallack, Gregory J., 2001, Soils of the past: An introduction to paleopedology, Second Edition, Blackwell Science Ltd., Oxford, England, 395 p.

Retallack, Gregory J., 1997, Fossil soils and their role in Devonian global change: Science, v. 276, p. 583-585.

Retallack, Gregory J., 1983, Late Eocene and Oligocene paleosols from Badlands National Park, South Dakota: Geological Society of America Special Paper no. 193, 82 p.

Ricketts, B.D., 1991, Lower Paleocene drowned valley and barred estuaries, Canadian Artic Islands: aspects of their geomorphological and sedimentological evolution: In Smith, D.G., Reinson, G.E., Zaitlin, B.A., and Rahmani, R.A. (eds.), Clastic tidal sedimentology, Canadian Society of Petroleum Geologists Memoir 16, Calgary, Alberta, p. 91-106

Scheckler, S.E., Postnikoff, D.L.L., Chameroy, E.J., 2000, Late Devonian forests with the first large trees (Archaeopteris), abstract from 2000 Botany Conference New Frontiers in Botany, American Journal of Botany Supplement, v. 87, no. 6.

Schieber, J., 1999, Distribution and deposition of mudstone facies in the Upper Devonian Sonyea Group of New York. Journal of Sedimentary Research, v. 69, p. 909-925.

Slingerland, R., and Loule, J.P., 1988, Wind/wave and tidal processes along the Upper Devonian Catskill shoreline in Pennsylvania, U.S.A.: In McMillan, N.J., Embry, A.F., and Glass, D.J. (eds.), Devonian of the world: Volume II: Sedimentation, Proceedings of the second international symposium on the Devonian system, Canadian Society of Petroleum Geologists, Calgary, Alberta, Canada, p. 125-138.

Smith, Derald G., 1988, Tidal bundles and mud couplets in the McMurray Formation, Northeastern Alberta, Canada: Bulletin of Canadian Petroleum Geology, v. 36, no. 2, p. 216-219.

Smith, Derald G., 1985, Modern analogues of the McMurray Formation channel deposits, sedimentology of mesotidal-influenced meandering river point bars with inclined beds of alternating mud and sand: Alberta Oil Sands Technology and Research Authority, Final Report for Research Project No. 391, Calgary, 78 p.

Soil Survey Staff, 1996, Keys to soil taxonomy, Seventh Edition, United States Department of Agriculture, Natural Resources Conservation Service, 644 p.

Swift, D.J.P., 1984, Response of the shelf floor to flow: In R.W. Tillman, D.J.P Swift, and R.G. Walker (eds.), Shelf sands and sandstone reservoirs, SEPM short course no. 13, San Antonio, Texas, p. 135-224.

Sutton, R.G., Bowen, Z.P., and McAlester, A.L., 1970, Marine shelf environments of the Upper Devonian Sonyea Group of New York: GSA Bulletin, v.81, p. 2975-2992.

Thayer, C.W., 1974, Marine Paleoecology in the Upper Devonian of New York: Lethaia, v. 7, p. 121-155.

Thomas, R.G., Smith, D.G., Wood, J.M., Visser, J., Caverley-Range, E.A., and Koster, E.H., 1987, Inclined heterolithic stratification- Terminology, description, interpretation, and significance: Sedimentary Geology, v. 53, p. 123-179.

Thoms, R.E., and Berg, T.M., 1985, Interpretation of bivalve trace fossils in fluvial beds of the basal Catskill Formation (late Devonian), eastern U.S.A.: In Curran, H.A. (ed.), Biogenic structures: their use in interpreting depositional environments, Society of Economic Paleontologists and Mineralogists Special Publication 35, p. 13-21.

Van Den Berg, Jan H., 1981, Rhythmic seasonal layering in a mesotidal channel fill sequence, Oosterschelde Mouth, the Netherlands: Special Publications of the International Association of Sedimentology, v. 5, p. 147-159.

Williams, C.A., and Krause, F.F., 2000, Paleosol chronosequences and peritidal deposits of the Middle Devonian (Giventian) Yahatinda Formation, Wasootch Creek, Alberta, Canada, Bulletin of Canadian Petroleum Geology, v. 48, no. 1, p. 1-18.

Williams, G.E., 1991, Upper Proterozoic tidal rhythmites, South Australia: Sedimentary features, deposition, and implications for the earth's paleorotation: In Smith, D.G., Reinson, G.E., Zaitlin, B.A., and Rahmani, R.A., Clastic tidal sedimentology, Canadian Society of Petroleum Geologists Memoir 16, Calgary, Alberta, p. 161-178.

FIELD TRIP ROAD LOG

Cumulative Mileage	Miles From Last Point	Route Description
0.0	0.0	Mileage begins from the Hunt Union parking lot on the SUNY Oneonta campus. Make a right out of the parking lot and proceed to stop sign (bear left).
0.1	0.1	Make a left onto Ravine Parkway and proceed 0.6 miles to stop sign.
0.7	0.6	Make a left onto West Street. Proceed down hill for 0.7 miles to traffic light.
1.4	0.7	Make a left at traffic light onto Chestnut Street. Proceed 0.3 miles to second traffic light.
1.7	0.3	Make a right at traffic light onto Main Street. Proceed 0.5 miles to Junction I-88.
2.2	0.5	Make a right onto Interstate I-88 Exit 14 on-ramp heading westbound. Proceed 17.3 miles to exit 10.
19.5	17.3	Take exit 10 off I-88 at Unadilla.
20.1	0.6	As you descend off of long off-ramp, bear left. Make your first left onto River Road located just before bridge over Susquehanna River. Proceed on River Road to the second road on the left.
21.1	1.0	Make a hard left onto Delaware County Route 23 heading eastbound. Proceed to the third road on the right.
22.3	1.2	Turn right onto Dunshee Road. Proceed up mountain for entire length of Dunshee Road to stop sign.
23.9	1.6	Turn right onto Delaware County Route 35. Proceed up hill to first road on the left.

Cumulative Mileage	Miles From Last Point	Route Description
24.3	0.4	Turn left onto Skytop Lane and proceed to dead end.
24.6	0.3	At dead end, park in dirt parking area near gate entrance to **STOP #1- SKYTOP LANE QUARRY (outcrop 43).** See text for descriptions and interpretations of facies T_{xb}-td, T_{xb}-ti, P_{bms}, and H_b-i, and paleosols P_p and P_{ao}.
24.9	0.3	Return to intersection of Skytop Lane and Delaware County Route 35, Turn right onto CR 35. Proceed 1.5 miles on Delaware County Route 35 to Village of Sidney Center .
26.4	1.5	Turn left onto Maywood Lane (Historical Depot Drive).
26.5	0.1	Proceed up hill to Maywood Historical Depot parking area. Eat lunch and attend optional tour of Historical Railroad Depot.
26.6	0.1	Return to intersection of Maywood Lane and CR 35. Turn right onto CR35. Proceed 3.0 miles on CR 35.
29.6	3.0	You will see a small lake on your left. Turn left onto Cummings Road and proceed 0.6 miles.
30.2	0.6	Turn right onto gravel access road to **Sheetz Quarry (outcrop 51) = STOP #2.** Follow gravel access road 0.5 miles to gate
30.7	0.5	Park at gate and proceed on foot to quarry
31. 2	0.5	Return to Cummings Road and turn left. Proceed 0.6 miles on Cummings Road.
31.8	0.6	Turn left onto CR 35 and proceed 3.5 miles to intersection with NYS Route 206.

Cumulative Mileage	Miles From Last Point	Route Description
35.3	3.5	Make a right onto NYS Route 206. Proceed 1.4 miles to the Hamlet of Masonville
36.7	1.4	Make a right at stop sign onto NYS Route 8 North. Proceed 3.2 miles on NYS Route 8 to Delaware County Route 4.
39.9	3.2	Make a right onto CR 4. Proceed to stop sign at intersection with Cole Road spur.
40.0	0.1	Continue straight up hill to Sidney Mountain Quarry access road.
40.2	0.2	Bear left onto gravel access road and follow to entrance gate for Sidney Mountain Quarry. Park on side of access road and proceed on foot to quarry.
40.3	0.1	**STOP #3 Sidney Mountain Quarry (outcrop 6)**

Return to intersection of CR4 and NYS Route 8 and turn right onto 8 North to reach I-88.

APPENDIX I: LOCATIONS OF SONYEA OUTCROPS USED IN THIS STUDY

OUTCROP NUMBER	LOCATION	QUADRANGLE	LATITUDE	LONGITUDE	ELEVATION (Ft AMSL)	ASSIGNED FACIES	MAGNAFACIES/ FORMATION
1	Interstate-88 at Exit 8, Bainbridge	Sidney	42°17' 37"	75°27' 51"	1180	HS_{cs}	Chemung/Triangle
2	Route 8, Sidney	Sidney	42°17' 14"	75°23' 52"	1420	HS_{cs}/ S_{dg}	Chemung/Glen Aubrey-Sawmill Creek
3	Thorpe Road at Route 8, Sidney	Sidney	42°16' 50"	75°23' 51"	1600	HS_{cs}/S_{dg}/ HS_{cs}-A	Chemung/Glen Aubrey-Sawmill Creek
4	Route 8 near Bundy Hollow Road, Sidney	Sidney	42°15' 46"	75°23' 56"	1400	HS_{cs}	Chemung/Glen Aubrey-Sawmill Creek
5	Delaware County Route 4, Sidney	Sidney	42°17' 14"	75°23' 29"	1460	HS_{cs}	Chemung/Glen Aubrey
6 = STOP #3	**Sidney Mountain Quarry, Delaware County Route 4, Sidney**	Sidney	42°16' 35"	75°23' 20"	1779	P_{bms}/ H_b-sl/ H_b-i/P_{gp}/ P_{aa}/ S_{dg} /HS_{cs}	Cattaraugus/ Unnamed Fm and Chemung/Glen Aubrey
7	Pine Hill Road, Sidney	Unadilla	42°17' 30"	75°21' 50"	1851	T_{xb}-td	Cattaraugus/Lower Walton
8	Dunshee Road Quarry, Sidney Center	Unadilla	42°17' 06"	75°17' 08"	1720	HS_{cs}-A	Chemung/Glen Aubrey
9	Dunshee Hill, Steele Pasture Quarry, Sidney Center	Unadilla	42°17' 13"	75°16' 58"	1728	HS_{cs}/ S_{dg}/ HS_{cs}-A	Chemung/Glen Aubrey-Sawmill Creek
10	Dunshee Hill, Outcrop A, Sidney Center	Unadilla	42°17' 32"	75°17' 02"	1745	T_{xb}-td	Chemung/Glen Aubrey
11	Dunshee Hill, Outcrop B, Sidney Center	Unadilla	42°17' 30"	75°16' 57"	1760	T_{xb}-td	Cattaraugus/ Unnamed Fm
12	Dunshee	Unadilla	42°17' 29"	75°16' 55"	1787	T_{xb}-td	Cattaraugus/

	Hill, Outcrop C, Sidney Center						Unnamed Fm
13	Dunshee Hill, Outcrop D, Sidney Center	Unadilla	42°17' 32"	75° 16' 49"	1790	T_{xb}-td	Cattaraugus/ Unnamed Fm
14	Dunshee Hill, Outcrop E, Sidney Center	Unadilla	42° 17' 35"	75° 16' 48"	1748	T_{xb}-td	Cattaraugus/ Unnamed Fm
15	Dunshee Hill, Outcrop F, Sidney Center	Unadilla	42° 17' 25"	75° 16' 38"	1768	T_{xb}-td	Cattaraugus/ Unnamed Fm
16	Dunshee Hill, Outcrop G, Sidney Center	Unadilla	42°17' 32"	75° 16' 44"	1850	T_{xb}-td	Cattaraugus/ Unnamed Fm
OUTCROP NUMBER	**LOCATION**	**QUADRANGLE**	LATITUDE	**LONGITUDE**	*ELEVATION* **(Ft AMSL)**	**ASSIGNED FACIES**	**MAGNAFACIES/ FORMATION**
18	Dunshee Hill, Outcrop I, Sidney Center	Unadilla	42°17' 33"	75° 16' 43"	1775	T_{xb}-td	Cattaraugus/ Unnamed Fm
19	Dunshee Hill, Outcrop J, Sidney Center	Unadilla	42° 17' 34"	75° 16' 44"	1769	T_{xb}-td	Cattaraugus/ Unnamed Fm
20	Dunshee Hill, Outcrop K, Sidney Center	Unadilla	42°17' 27"	75° 16' 36"	1774	T_{xb}-td	Cattaraugus/ Unnamed Fm
21	Dunshee Hill, Outcrop L, Sidney Center	Unadilla	42° 17' 29"	75° 16' 36"	1820	T_{xb}-td/ P_{bms}	Cattaraugus/ Unnamed Fm
22	Dunshee Hill, Outcrop M, Sidney Center	Unadilla	42° 17' 21"	75° 16' 20"	1795	T_{xb}-td	Cattaraugus/ Unnamed Fm
23	Dunshee Hill, Outcrop N, Sidney Center	Unadilla	42° 17' 25"	75° 16' 36"	1775	T_{xb}-td	Cattaraugus/ Unnamed Fm
24	Delaware County	Unadilla	42°16' 56"	75° 16' 52"	1880	P_{bms}	Cattaraugus/ Unnamed Fm

	Route 35, Outcrop O, Sidney Center						
25	Delaware County Route 35, Outcrop P, Sidney Center	Unadilla	42° 16' 53"	75° 16' 52"	1875	P_{bms}	Cattaraugus/ Unnamed Fm
26	Delaware County Route 35, Outcrop Q, Sidney Center	Unadilla	42°16' 40"	75° 17' 00"	1880	P_{bms}	Cattaraugus/ Unnamed Fm
27	Dunshee Hill, Outcrop R, Sidney Center	Unadilla	42° 17' 15"	75° 16' 47"	1762	HS_{cs}-A	Chemung/Glen Aubrey
28	Dunshee Hill, Outcrop S, Sidney Center	Unadilla	42°17' 15"	75° 16' 44"	1756	HS_{cs}-A	Chemung/Glen Aubrey
29	Dunshee Hill, Outcrop T, Sidney Center	Unadilla	42° 17' 18"	75° 16' 48"	1773	T_{xb}-ti	Cattaraugus/ Unnamed Fm
30	Dunshee Hill, Outcrop U, Sidney Center	Unadilla	42° 17' 16"	75° 16' 51"	1760	HS_{cs}-A	Chemung/Glen Aubrey
31	Dunshee Hill, Outcrop V, Sidney Center	Unadilla	42° 17' 14"	75° 16' 55"	1739	HS_{cs}-A	Chemung/Glen Aubrey
32	Dunshee Hill, Quarry 1, Sidney Center	Unadilla	42°17' 21"	75° 16' 52"	1799	P_{bms}	Cattaraugus/ Unnamed Fm
33	Dunshee Hill, Quarry 2, Sidney Center	Unadilla	42°17' 24"	75° 16' 48"	1825	P_{bms}	Cattaraugus/ Unnamed Fm
34	Dunshee Hill, Quarry 3, Sidney Center	Unadilla	42° 17' 25"	75° 16' 44"	1845	H_b-i/ T_{xb}-ti	Cattaraugus/ Unnamed Fm
35	Dunshee Hill, Quarry 4, Sidney	Unadilla	42° 17' 26"	75° 16' 41"	1836	P_{bms}/ H_b-i	Cattaraugus/ Unnamed Fm

	Center						
36	Dunshee Hill, Quarry 5, Sidney Center	Unadilla	42°17’ 29”	75° 16’ 39”	1836	P_{bms}/ H_b-i	Cattaraugus/ Unnamed Fm
38	Delaware County Route 35, Outcrop V, Sidney Center	Unadilla	42° 17’ 14”	75° 16’ 55”	1739	HS_{cs}	Chemung/Glen Aubrey
OUTCROP NUMBER	**LOCATION**	**QUADRANGLE**	LATITUDE	**LONGITUDE**	*ELEVATION* **(Ft AMSL)**	**ASSIGNED FACIES**	**MAGNAFACIES/ FORMATION**
40	Delaware County Route 35, Outcrop X, Sidney Center	Unadilla	42° 16’ 24”	75° 17’ 01”	1880	HS_{cs}/ S_{dg}	Chemung/Glen Aubrey-Sawmill Creek
41	Roof Road, Outcrop Y, Sidney Center	Unadilla	42°16’ 33”	75° 15’ 35”	1480	HS_{cs}/ S_{dg}	Chemung/Glen Aubrey-Sawmill Creek
42	Roof Road, Outcrop Z, Sidney Center	Unadilla	42°16’ 21”	75° 16’ 09”	1720	T_{xb}-ti	Cattaraugus/ Unnamed Fm
43 = STOP #1	**Skytop Lane Quarry, Skytop Lane, Sidney Center**	Unadilla	42°16’ 53”	75° 16’ 20”	1851	P_{bms}/ H_b-i/ P_{ao}/P_{bo}/P_p/ T_{xb}-ti	Cattaraugus/ Unnamed Fm
44	Skytop Lane, Outcrop AA, Below Skytop Lane Quarry, Sidney Center	Unadilla	42° 16’ 59”	75° 16’ 26”	1750	T_{xb}-td	Cattaraugus/ Unnamed Fm
45	Skytop Lane Spur, Outcrop BB, Sidney Center	Unadilla	42° 16’ 30”	75° 16’ 23”	1680	H_b-i/ T_{xb}-ti	Cattaraugus/ Unnamed Fm
46	Skytop Lane Spur, Outcrop CC, Sidney Center	Unadilla	42°16’ 28”	75° 16’ 24”	1720	T_{xb}-td	Cattaraugus/ Unnamed Fm
47	Delaware County Route 35,	Unadilla	42°16’ 16”	75° 17’ 14”	1880	T_{xb}-ti/P_p	Cattaraugus/ Unnamed Fm

	Outcrop DD, East Masonville						
48	Unnamed Quarry, Wilcox Road at Olmstead Road, East Masonville	Unadilla	42°16' 32"	75°19' 03"	1860	P_{bms}/P_{aa}	Cattaraugus/ Unnamed Fm
49	Turner Quarry, Olmstead Road, East Masonville	Unadilla	42°16' 30"	75°18' 44"	1880	P_{bms}	Cattaraugus/ Unnamed Fm
50	Stanton Quarry, Olmstead Road, East Masonville	Unadilla	42°16' 44"	75°18' 26"	1720	T_{xb}-td/ P_{bms}	Cattaraugus/ Unnamed Fm
51 = STOP #2	**Sheetz Quarry, Cummings Road, East Masonville**	Unadilla	42°15' 10"	75°18' 29"	1909	P_{bms} /H_b-i	Cattaraugus/ Unnamed Fm
52	Cardi Quarry, Cummings Road, East Masonville	Unadilla	42°14' 51"	75°18' 09"	1960	P_{bms}	Cattaraugus/ Unnamed Fm
53	Delaware County Route 27, Sidney Center	Unadilla	42°15' 39"	75°15' 52"	1932	T_{xb}-ti/ P_{aa}/P_{gp}	Cattaraugus/ Unnamed Fm